DocuSign Envelope ID: F86F5BB6-506C-473A-87C5-368976444062

Distribution Agreement

In presenting this thesis or dissertation as a partial fulfillment of the requirements for an advanced degree from Emory University, I hereby grant to Emory University and its agents the non-exclusive license to archive, make accessible, and display my thesis or dissertation in whole or in part in all forms of media, now or hereafter known, including display on the world wide web. I understand that I may select some access restrictions as part of the online submission of this thesis or dissertation. I retain all ownership rights to the copyright of the thesis or dissertation. I also retain the right to use in future works (such as articles or books) all or part of this thesis or dissertation.

Signature: DocuSigned by: B72A6D8AF1D9406...

Mackenzie Prichard
Name

12/11/2023 | 4:19 PM EST
Date

DocuSign Envelope ID: F86F5BB6-506C-473A-87C5-368976444062

Title Distinct roles for expression of vasoactive intestinal peptide in the behavioral polymorphism in white-throated sparrows (Zonotrichia albicollis)

Author Mackenzie Prichard

Degree Doctor of Philosophy

Program Psychology

Approved by the Committee

DocuSigned by:
D65CCEB74BFF468...

Donna Maney
Advisor

DocuSigned by:
DD3286B34F954F7...

Aubrey Kelly
Committee Member

DocuSigned by:
5CEAD74D016043C...

Irwin Waldman
Committee Member

DocuSigned by:
B4345BEC9BC04A7...

Robert Hampton
Committee Member

DocuSigned by:
AC4A3A9E9ED1450...

Brent Horton
Committee Member

Committee Member

Accepted by the Laney Graduate School:

_____
Kimberly Jacob Arriola, Ph.D, MPH
Dean, James T. Laney Graduate School

_____
Date

Distinct roles for expression of vasoactive intestinal peptide in the behavioral polymorphism in white-throated sparrows (*Zonotrichia albicollis*)

By

Mackenzie R. Prichard

B.S., University of Montana
M.A., Emory University

Adviser: Donna L. Maney, Ph.D.

An abstract of
A dissertation submitted to the Faculty of the
James T. Laney School of Graduate Studies of Emory University
in partial fulfillment of the requirements for the degree of
Doctor of Philosophy
in Psychology
2023

Abstract

Distinct roles for expression of vasoactive intestinal peptide in the behavioral polymorphism in white-throated sparrows (*Zonotrichia albicollis*)

By Mackenzie R. Prichard

Understanding how behavioral traits are inherited and, to some extent, genetically encoded is critical to understanding how behavior evolves. Investigating the genetic basis of behavior is often challenging because behavioral traits are highly plastic and multiply determined. Model organisms that carry supergenes have garnered attention for their utility in this pursuit. One such organism is the white-throated sparrow (*Zonotrichia albicollis*), which stands out among others because half the population carries one of the largest chromosomal inversions, or supergenes, discovered to date. This supergene forms the basis of a behavioral polymorphism that represents a life history trade-off; individuals with the supergene are more aggressive and less parental than those without it. In this study, I looked for evidence that the neuromodulator vasoactive intestinal peptide (VIP), which is encoded by a gene inside the supergene, is associated with multiple aspects of the behavioral polymorphism in white-throated sparrows. Previous research in other avian species demonstrated that VIP in the anterior hypothalamus (AH) promotes aggression, whereas VIP released by neurons in the infundibular nucleus (IN) controls the secretion of prolactin, a parenting hormone. Here, I demonstrate that expression of *VIP* mRNA in the AH is greater in birds that carry the supergene than in those that do not and that in the IN, the birds that do not carry the supergene have higher levels of expression than those that do. I show that the supergene allele of *VIP* is expressed more than the standard allele in both brain regions, but the degree that the supergene allele is overexpressed is greater in the AH than in the IN. I also demonstrate that both the level of *VIP* expression overall and the degree to which the supergene allele is overexpressed in the AH and the IN predict aggression and parental care, respectively. I conclude by discussing several mechanisms that could affect *VIP* expression and propose how *VIP* may interact with larger neural and gene expression networks that mediate life history trade-offs.

Distinct roles for expression of vasoactive intestinal peptide in the behavioral polymorphism in white-throated sparrows (*Zonotrichia albicollis*)

By

Mackenzie R. Prichard

B.S., University of Montana
M.A., Emory University

Adviser: Donna L. Maney, Ph.D.

A dissertation submitted to the Faculty of the
James T. Laney School of Graduate Studies of Emory University
in partial fulfillment of the requirements for the degree of
Doctor of Philosophy
in Psychology
2023

Acknowledgments

I want to thank my adviser, Dr. Donna Maney, for her mentorship, support, and patience over the years. I also want to thank the members of my dissertation committee for their advice and guidance through this research. Also, thank you to Paula Mitchell and all of the faculty, students, and staff in the psychology department, who helped me along the way. My project was also hugely supported by the extended family of the “Birdbrain” lab. I want to thank Isabel Fraccaroli and Erik Iverson for their direct involvement with data collection and troubleshooting, Irfan and Reeya for scoring so many hours of videos, as well as all of the field technicians who helped me in Minnesota (Lauren Chronnister, Wren Corvus, Edwin Harris, Michelle Moyer, Emilia Skogen, and Rachel Weisbeck). Thanks also to my original lab sibling, Natalie Pilgeram, Dr. Nicole Baran, and especially Dr. Jenny Merritt, who was so kind, so knowledgeable, and always there to help. I’m also grateful to my undergraduate mentors, particularly Dr. Creagh Breuner, for supporting and encouraging me to pursue this degree.

I also want to express my gratitude to Boulder Lake Environmental Learning Center for sharing their space and property with us to conduct research in the field. I want to express my respect for the Chippewa Tribe of the Ojibwe Nation, who were the ancestral stewards of the land where my sparrows lived, and for the Muscogee people, who were the ancestral stewards of the land where Emory was built.

I am also so grateful to my family, who love and support me with all their might from so many, many miles away. I'm thankful for all my friends who helped keep things in perspective and for all the great memories we made during this unique time of my life. Last but not least, I want to thank my dog, Ezra, the sweetest, goofiest, noisiest little man on three legs.

Table of Contents

List of Tables i

List of Figures ii

List of Symbols and Abbreviations iii

Introduction 1

Results 8

Discussion 16

Methods 27

References 38

Figures 57

Appendix 69

List of Tables

Table S1.	Sample sizes within year, breeding stage, morph, and sex.	70
Table S2.	Morph differences in aggressive/territorial behaviors other than singing.	71
Table S3.	Morph differences in and correlations between territorial singing and *VIP* expression.	73
Table S4.	Allelic imbalance in the AH.	74
Table S5.	Morph differences in parental behaviors other than nestling provisioning.	75
Table S6.	Morph differences in and correlations between nestling provisioning and *VIP* expression.	77
Table S7.	Allelic imbalance in the IN.	78
Table S8.	Interactions between morph, sex, and brain region in *VIP* expression.	79
Table S9.	Nucleotide sequences of primers and probes for RT-qPCR assays.	80

List of Figures

Figure 1.	The white-striped (WS) and tan-striped (TS) morphs and their chromosomes.	57
Figure 2.	Morph differences in territorial singing and vasoactive intestinal peptide (*VIP*) expression in the anterior hypothalamus (AH), and the correlation between the two, in free-living white-throated sparrows.	58
Figure 3.	Allelic imbalance in the AH of the pre-parental cohort.	59
Figure 4.	Morph differences in nestling provisioning and vasoactive intestinal peptide (*VIP*) expression in the infundibular nucleus (IN), and the correlation between the two, in free-living white-throated sparrows.	61
Figure 5.	Allelic imbalance in the IN of the parental cohort.	62
Figure 6.	Morph differences in *VIP* expression depended on brain region.	64
Figure 7.	*VIP* expression in the AH and IN were negatively correlated.	65
Figure 8.	Allelic imbalance in VIP expression differs between the AH and IN.	66
Figure 9.	Correlation between allelic imbalance and overall expression of *VIP* in the AH with the cohorts pooled.	67
Figure 10.	Correlation between allelic imbalance and overall expression of *VIP* in the IN with the cohorts pooled.	68
Figure S1.	Correlation between *VIP* expression in the IN and territorial singing.	81
Figure S2.	Correlation between allelic imbalance in the IN and territorial singing.	82
Figure S3.	Correlation between *VIP* expression in the AH and nestling provisioning.	83
Figure S4.	Correlation between allelic imbalance in the AH and nestling provisioning.	84
Figure S5.	Correlation between allelic imbalance and overall *VIP* expression in the AH within the parental cohort.	85
Figure S6.	Correlation between allelic imbalance and overall *VIP* expression in the IN within the pre-parental cohort.	86
Figure S7.	Anatomical locations of punches of the anterior hypothalamus and infundibular nucleus.	87
Figure S8	Standard curve used for the assay of allelic imbalance ($ZAL2^m$: ZAL2).	88

List of Symbols and Abbreviations

ΔCp	delta crossing point
AC	anterior commissure
AH	anterior hypothalamus
AVM	ventromedial arcopallium
AR	androgen receptor
AR	gene encoding androgen receptor
cDNA	complementary DNA
cAMP	cyclic adenosine monophosphate
Cp	crossing point
Cp_{ref}	mean Cp of each gene or primer/probe
Cy5	cyanine
D1	dopamine receptor 1
DRD1	gene encoding dopamine receptor 1
D2	dopamine receptor 2
DRD2	gene encoding dopamine receptor 2
E	efficiency
ESR1	gene encoding estrogen receptor 1 (i.e., estrogen receptor α)
ERα	estrogen receptor α
FAM	fluorescein
GAPDH	glyceraldehyde 3-phosphate dehydrogenase
gDNA	genomic DNA
HKG	housekeeping gene
ICC	interclass correlation coefficient
IN	infundibular nucleus of the hypothalamus

INDEL	insertion/deletion polymorphism
m	slope
Mb	megabases (e.g., of nucleotides in DNA)
mRNA	messenger ribonucleic acid
ME	median eminence
PCR	polymerase chain reaction
PPIA	peptidylprolyl isomerase A
RT-qPCR / qPCR	real-time quantitative polymerase chain reaction
RQ	relative quantity
RQR	ratio of the relative quantity of allele/probe
SNP	single nucleotide polymorphism
STI	simulated territorial intrusion
TS	tan-striped
TSF	tan-striped female
TSM	tan-striped male
UTR	untranslated region
VIP	vasoactive intestinal peptide
VIP	gene encoding vasoactive intestinal peptide
VIP^{2}	ZAL2 allele of vasoactive intestinal peptide
VIP^{2m}	$ZAL2^{m}$ allele of vasoactive intestinal peptide
WS	white-striped
WSF	white-striped female
WSM	white-striped male
ZAL2	chromosome 2 of *Zonotrichia albicollis*
$ZAL2^{m}$	metacentric version of chromosome 2 of *Zonotrichia albicollis*

Introduction

As with any evolvable trait, a crucial part of understanding how a behavioral trait evolves is understanding how it is inherited and, thus, to some extent, genetically encoded. Understanding the genetic basis of behavior is challenging because behavioral traits are highly plastic and multiply determined. One way that complex traits like behavioral traits might be genetically encoded is through clusters of tightly linked loci or supergenes (Charlesworth, 2016; Schwander et al., 2014; Thompson & Jiggins, 2014). The resulting linkage disequilibrium, which is characteristic of supergenes, allows genomic changes that benefit a complex phenotype to accumulate within a single, heritable unit. This phenomenon presents an opportunity for multiple complex phenotypes to be maintained stably even in interbreeding populations though processes such as disruptive selection and non-random mating (Mather, 1955; Sinervo & Svennson, 2002). Supergenes that contribute to complex traits have been discovered in many taxa, including intricate coloration mimicry in butterflies (Nishikawa et al., 2015), colony queen number and social organization in ants (Purcell et al., 2021), and alternative behavioral morphs in birds (Maney & Küpper, 2022).

Among the species that carry supergenes that affect behavior, one example that stands out is the white-throated sparrow (*Zonotrichia albicollis*). White-throated sparrows are seasonally breeding, migratory songbirds endemic to eastern North America (Falls & Kopachena, 2020). In this species, a supergene on the second chromosome is directly linked to alternative behavioral phenotypes and plumage morphs (Figure 1). Individuals that comprise the white-striped (WS) morph carry the supergene (Thorneycroft, 1975), are more aggressive (Kopachena & Falls, 1993a; Horton et al., 2014b), and are less parental than tan-striped (TS) individuals (Knapton & Falls, 1983; Kopachena & Falls, 1993b). The two morphs are equally prevalent in both sexes

(Thorneycroft, 1975), and most breeding pairs are heteromorphic (i.e., one TS and one WS; Lowther, 1961; Tuttle et al., 2016). The supergene in WS birds is a result of a series of pericentric inversions that encompass ~100 Mb and ~1100 genes, which amounts to ~10% of the entire genome, making it one of the largest examples of a supergene discovered to date (Davis et al., 2011; Huynh et al., 2011; Thomas et al., 2008). TS birds are always homozygous for the standard version of chromosome two (ZAL2). In contrast, WS birds have at least one copy of $ZAL2^m$, a metacentric version of chromosome two containing the supergene (Thorneycroft, 1975). The vast majority of WS birds are heterozygous for $ZAL2^m$ ($ZAL2/ZAL2^m$). Homozygotes ($ZAL2^m/ZAL2^m$) are extremely rare, which is attributable to near-perfect disassortative mating between the morphs (Lowther, 1961; Tuttle et al., 2016). This combination of heterozygosity and disassortative mating makes the $ZAL2/ZAL2^m$ chromosome similar to many sex chromosomes, such as the human X/Y chromosomes (Campagna, 2016; Tuttle et al., 2016). And like in sex chromosomes, recombination between ZAL2 and $ZAL2^m$ is suppressed, and over time, the two chromosomes have diverged genetically (Davis et al., 2011; Huynh et al., 2011; Thomas et al., 2008).

The differences in behavior between the TS and WS morphs have been extensively characterized (reviewed by Maney et al., 2020). Although some morph differences in behavior have been reported in sparrows that were not in breeding condition (e.g., Barcelo-Serra et al., 2020), the behavioral polymorphism is most pronounced during breeding (Maney et al., 2009; Spinney et al., 2006; Watt et al., 1984). Many, if not most, of the behaviors that differ between the morphs are hormone dependent, and the morph differences in these behaviors are most prominent during breeding, when circulating levels of steroid hormones are elevated. These hormones, such as testosterone and estradiol, are generally associated with increased aggression

and sexual behavior in birds (Ball & Balthazart, 2004; Rosvall et al., 2012). During the breeding season, birds of the more aggressive WS morph have higher levels of testosterone and estradiol than TS birds (Grogan et al., 2019; Horton et al., 2014b; Spinney et al., 2006; Swett & Breuner, 2008). However, morph differences in aggression persisted after experimentally equalizing plasma levels of these hormones, indicating that the mechanism underlying the morph difference in aggression is more complex than can be explained by morph differences in plasma levels alone (Maney et al., 2009; Merritt et al., 2018). The gene that encodes estrogen receptor α, *ESR1*, is captured by the ZAL2^{m} inversion and is hypothesized to contribute to the morph difference in aggression (reviewed by Maney et al., 2008). *ESR1* is expressed more in WS birds than TS birds in the ventromedial arcopallium (AVM; previously called nucleus taeniae of the amygdala; Horton et al., 2016; Grogan et al., 2019; Mello et al., 2019). Using gene expression knockdown, Merritt et al. (2020) demonstrated that reducing the expression of *ESR1* in AVM in WS birds to the level expressed in TS birds reduced aggression in WS birds to the TS level. This result suggests that steroids and their receptors, particularly ERα, could play an essential part in the alternative behavioral phenotypes. Still, the polymorphism in white-throated sparrows extends beyond aggression and is likely the result of numerous factors related to the ZAL2^{m} inversion (reviewed by Maney et al., 2015).

A near neighbor to *ESR1* within the ZAL2^{m} supergene is the gene encoding vasoactive intestinal peptide, or *VIP*. *VIP* was named for its role in blood flow to the gut (Klimaschewski, 1997), but it is also a neuropeptide that is expressed in the avian brain (Kuenzel & Blähser, 1994; Kuenzel et al., 1997; Montagnese et al., 2015), particularly in brain regions that make up a well-studied circuit of brain regions known as the ‘social behavior network’ (Goodson, 2005). Furthermore, *VIP* expression is associated with a variety of social behaviors, including

aggression (reviewed by Kingsbury, 2015). *VIP* expression in the anterior hypothalamus (AH) correlated positively with aggression in song sparrows (*Melospiza melodia*) and field sparrows (*Spizella pusilla*; Goodson et al., 2012b) and experimental knock-down of *VIP* expression in this region reduced aggression in two species of finch (*Taeniopygia guttata* and *Uraeginthus granatina*), suggesting VIP in the AH is causal for aggression in some passerines (Goodson et al., 2012a). In white-throated sparrows, we previously demonstrated using *in situ* hybridization that *VIP* expression in the AH was higher in WS birds than in TS birds and positively predicted territorial singing in both morphs (Horton et al., 2020a). Thus, increased *VIP* expression in the AH of WS birds could play a role in increased levels of aggressive behavior in the WS morph relative to the TS morph. In this study, I measured aggression and *VIP* expression in free-living white-throated sparrows in breeding condition. I predicted that, as demonstrated previously, (1) WS birds would be more aggressive than TS birds, (2) *VIP* expression in the AH would be higher in WS birds than TS birds, and (3) *VIP* expression in the AH would correlate positively with aggressive behavior in both morphs. These results would provide evidence consistent with the hypothesis that *VIP* expression in the AH contributes to morph differences in aggression.

In addition to its role in aggression, VIP also plays a role in parental care (reviewed by Kingsbury, 2015). VIP neurons in the infundibular nucleus of the hypothalamus (IN) project to the base of the brain, where they secrete VIP into the portal vasculature (reviewed by Smiley, 2019). The VIP then acts on the anterior pituitary to stimulate the expression (Talbot et al., 1991; Xu et al., 1996) and release of prolactin (El Halawani et al., 1990; El Halawani et al., 2000; Kulick et al., 2005; Macnamee et al., 1986; Maney et al., 1999; reviewed by Smiley, 2019). In turkeys and bantam hens, for example, immunization against VIP completely blocked prolactin secretion, whereas infusion of VIP stimulated it (Talbot et al., 1991; Youngren et al., 1996;

Youngren et al., 1998). Prolactin is a taxonomically well-conserved hormone that contributes to many behaviors and physiological changes associated with parental care across vertebrates (Bole-Feysot et al., 1998; Smiley, 2019). In birds, elevated prolactin secretion corresponds with periods during which the demands of parenthood are most intense (Farrar et al., 2022; Goldsmith, 1982; Smiley & Adkins-Regan, 2016), and *VIP* expression in the IN mirrors these seasonal changes (Chaiseha et al., 1998; Kosonsiriluk et al., 2008; Sharp et al., 1998). In white-throated sparrows, Horton et al. (2020a) found that both *VIP* expression in the IN and nestling provisioning rates were higher in TS males than in WS males, which is consistent with the hypothesis that *VIP* expression in this region contributes to morph differences in parental behavior. In this study, I measured parental behavior and *VIP* expression in the IN of free-living white-throated sparrows that were engaging in provisioning offspring. I predicted that (1) TS birds would be more parental than WS birds, (2) *VIP* expression in the IN would be higher in TS birds than WS birds, and (3) *VIP* expression in the IN would correlate positively with parental behavior in both morphs. These results would provide evidence consistent with the hypothesis that *VIP* expression in the IN contributes to morph differences in parental behavior.

Thus far, I have reviewed evidence demonstrating potentially distinct roles for *VIP* expression in two behaviors relevant to the behavioral polymorphism in white-throated sparrows. In this species and others, *VIP* expression in the AH appears to promote aggression, while *VIP* expression in the IN may promote parental care. Kingsbury et al. (2015) expanded on these observations in male zebra finches (*Taeniopygia guttata*). They demonstrated that *VIP* expression in a region containing the IN correlated positively with time spent in the nest, consistent with the known role of VIP in this region as the primary releasing factor for prolactin in birds (reviewed by Kingsbury, 2015 and Smiley, 2019). However, in the AH, *VIP* expression

correlated negatively with time spent in the nest (Kingsbury et al., 2015). This additional context led to the hypothesis that VIP in these two brain regions contributes to a trade-off between parental and aggressive life history strategies (reviewed by Kingsbury & Wilson, 2016). These alternative life history strategies are exemplified by the behavioral phenotypes of the WS and TS morphs in white-throated sparrows (Maney, 2008; Tuttle, 2003). Therefore, in this study, I predicted that VIP expression in the two regions would reflect that behavioral trade-off; in the VIP cell population that promotes aggression, expression would be higher in the more aggressive morph; in the population that promotes parenting, it would be higher in the more parental morph. This result would provide evidence that the regulation of *VIP* expression differs between the AH and IN such that the morph difference changes direction between these two regions, which would be consistent with the hypothesis that VIP plays independent roles in aggression and parenting.

In white-throated sparrows, the presence or absence of the supergene forms the causal basis for the two alternative behavioral phenotypes. Importantly, genetic polymorphisms between the ZAL2 allele of *VIP* (VIP^2) and the ZAL2^m allele of *VIP* (VIP^{2m}) are accumulating almost exclusively in non-protein coding regions of the gene. Therefore, it is likely the *expression* of *VIP*, not its *function*, that has been affected by the divergence between ZAL2 and ZAL2^m. There is only one single nucleotide polymorphism (SNP) in the protein-coding sequence, and it does not affect the amino acid sequence of the active VIP protein (Sun et al., 2018). The genetic divergence in the non-protein-coding regions, however, could result in an important difference in *expression* between the VIP^2 and VIP^{2m} alleles, ultimately leading to morph differences in *levels* of VIP. In *cis*-regulatory regions, for example, even small genetic polymorphisms like the SNPs and insertion/deletion polymorphisms (INDELs) accumulating on

VIP^{2m} can have substantial effects on gene expression and, consequently, on phenotypes (Wittkopp & Kalay, 2011; Wray, 2007), including behavioral phenotypes (Niepoth & Bendesky, 2020). For example, mutations in a cAMP-responsive element located in the human *VIP* promoter abolished the expression of *VIP in vitro* (Hahm & Eiden, 1996). Mutations in *cis*-regulatory regions can also create and disrupt CpG dinucleotides and consequently affect methylation at those sites (Merritt et al., 2020; Okhovat et al., 2015; Okhovat et al., 2017), which can change expression, and thus behavior (Aristizabal et al., 2020; Bentz et al., 2021; Mamrut et al., 2013).

In white-throated sparrows, we previously reported that a putative cis-regulatory element within the *VIP* gene is less methylated on *VIP*^{2m} than *VIP*^{2} in a sample of the hypothalamus containing the AH (Prichard et al., 2022). Notably, this difference in methylation was not due to methylation at polymorphic CpG sites but instead was due to methylation at CpG sites that were shared between the two alleles (Prichard et al., 2022). Because methylation usually suppresses gene expression (Eden & Cedar, 1994), these results suggest that *VIP*^{2m} is likely to be overexpressed relative to *VIP*^{2} in the hypothalamus of WS birds. Differential expression of two alleles can be estimated by measuring the expression of one allele relative to the other; a ratio different from 1:1, that is, unequal expression of the alleles, is called allelic imbalance (e.g., Chen et al., 2008; Merritt et al., 2020). In this study, I measured allelic imbalance in *VIP* expression by quantifying the expression of *VIP*^{2m} relative to *VIP*^{2} in the AH and IN. Up- or downregulation of one allele relative to the other in WS birds may contribute to downstream morph differences in aggression and parental care, respectively.

Summary of introduction

Differential expression of *VIP* between the morphs in two key brain regions, the AH and

the IN, may contribute to alternative behavioral phenotypes in the white-throated sparrow. In this study, I quantified either aggression or parental care in free-living white-throated sparrows. Next, I measured *VIP* expression in the AH and IN of those animals. I predicted that the *VIP* expression in the AH would be greater in WS birds than in TS birds, and I expected that the opposite would be true in the IN (i.e., TS expression would be higher than WS in this region). I hypothesized that differential allele-specific expression contributes to the overall level of *VIP* expression within each brain region and thus may play a role in morph differences. To find evidence of differential expression of the alleles, I measured allelic imbalance in *VIP* expression in the AH and IN of WS birds. Because the behavioral phenotypes in white-throated sparrows are a good example of alternative life history strategies, the present study aimed to reveal patterns of differential expression of *VIP* in the AH and IN to shed light on the role VIP plays in life history trade-offs between aggression and parental care.

Results

Aggressive behavior and *VIP* expression in the AH

VIP expression in the AH is known to be positively correlated with and causal for aggression in several species of songbirds (Goodson et al., 2012a, b; Horton et al., 2020a). Here, because white-throated sparrows of the WS morph engage in more territorial aggression than their TS counterparts (e.g., Horton et al., 2014b), I hypothesized that WS birds would have higher levels of *VIP* expression in the AH. I predicted further that *VIP* expression in the AH would positively predict aggressive behavior independently of morph. I measured aggressive behavior and parental care (described in the next section) in two separate groups of free-living white-throated sparrows, a “pre-parental” cohort and a “parental” cohort (Table S1). I measured aggressive behavior in the pre-parental cohort during the breeding season, from early after

territory establishment and pairing at the breeding site until the start of incubation. To measure aggressive behavior, I used a behavioral assay called simulated territorial intrusion (STI). In these assays, two observers placed a caged, male conspecific decoy and a speaker playing conspecific song in the territory of a focal pair and recorded the behavioral response of the resident birds (Horton et al., 2014b). Although I measured and tested for morph differences in other behaviors observed during the STIs (Table S2), I focused my analyses on territorial singing because it is a predominate component of territorial aggression in this species and was previously shown to differ robustly between the morphs (Horton et al., 2014b; Kopachena & Falls, 1993a). As expected, I found that WS birds sang more often than TS birds in response to STI ($F_{(1,29)}$ = 97.82, $p < 0.001$; Figure 2A, Table S3).

To test the hypothesis that *VIP* expression in the AH is higher in WS than in TS birds, I used RT-qPCR to measure *VIP* expression in the AH tissue microdissected from the same animals evaluated for aggression. I found that *VIP* expression in the AH was greater in the WS morph than in the TS morph ($F_{(1,22)}$ = 8.289, $p = 0.009$; Figure 2B, Table S3). I next hypothesized that *VIP* expression in the AH would predict aggressive behavior independently of morph, and indeed, I found a positive correlation between *VIP* expression in the AH and territorial singing; the higher the level of *VIP* expression in the AH, the more frequently the individual sang in response to STI (R = 0.469, 95%CI [0.108, 0.720], $p = 0.014$; Figure 2C, Table S3). These findings were consistent with a previous study in which *VIP* expression was measured by *in situ* hybridization in a different population of white-throated sparrows (Horton et al., 2020a). Another previous study, in zebra finches, showed a negative correlation between aggression and *VIP* expression in the IN (Kingsbury et al., 2015). Here, I found that the correlation between *VIP* expression in the IN and singing was not statistically significant (R = -

0.069, 95%CI [-0.438, 0.319], p = 0.733; Figure S1, Table S3), and this relationship was significantly weaker than in the AH (Fisher's Z: p = 0.045). Altogether, my results demonstrate that the morph difference in aggressive behavior corresponds with a morph difference in *VIP* expression in the AH, and that *VIP* expression in the AH, but not the IN, significantly predicts territorial singing.

The ZAL2^{m} supergene captures the *VIP* gene, and variation in regulatory regions is accumulating between the ZAL2^{m} and ZAL2 alleles of *VIP* (Sun et al., 2018). Thus, differential expression of the two alleles may be partly responsible for the increased expression of *VIP* in the AH of WS birds. To test for differential expression of the alleles, I measured allelic imbalance using a multiplex RT-qPCR assay targeting a SNP in the 3'UTR. This approach enabled me to determine the ratio of the expression of the two *VIP* alleles in the AH and IN of WS birds. This assay was conducted only in WS birds because the TS birds are homozygous for ZAL2. I found that VIP^{2m} was overexpressed, relative to VIP^{2}, in the AH of WS birds (one-sample t-test: t > 7.6, p < 0.05; Figure 3A, Table S4). Next, I reasoned that if upregulation of VIP^{2m} expression in WS birds contributes to morph differences in *VIP* expression in the AH, then there should be a positive relationship between the degree of allelic imbalance and the overall expression of *VIP*. I found that, while not significant, the correlation between allelic imbalance and overall expression of *VIP* in the AH was positive, which was consistent with my hypothesis (R = 0.350, 95%CI [-0.249, 0.755], p = 0.241; Figure 3B, Table S4). Lastly, I reasoned that if upregulation of VIP^{2m} expression in WS birds contributes to morph differences in aggression, then allelic imbalance in the AH would also correlate positively with territorial singing. I found a positive correlation, which trended significant, between the degree of allelic imbalance in the AH and territorial singing (R = 0.482, 95%CI [-0.040, 0.797], p = 0.069; Figure 3C, Table S4). In contrast, I found

no correlation between territorial singing and the degree of allelic imbalance in the IN (R = 0.021, 95%CI [-0.464, 0.497], p = 0.937; Figure S2, Table S4). However, territorial singing was not more strongly correlated with the degree of allelic imbalance in the AH than in the IN (Fisher's Z: p = 0.200).

Parental care and *VIP* expression in the IN

The aggressive behavioral phenotype of the WS morph is complimented by the parental behavioral phenotype of the TS morph; TS birds tend to engage in parental behaviors like nestling provisioning more than WS birds (Kopachena & Falls, 1993b; Knapton & Falls, 1983). Because VIP is the primary releasing factor for prolactin, which can promote parental behavior (reviewed by Smiley, 2019), I hypothesized that *VIP* expression would be higher in the IN of TS birds than in WS birds and that *VIP* expression in this region would correlate positively with nestling provisioning when statistically controlling for morph. I tested these hypotheses in the parental cohort, which comprised animals collected later in the breeding season than the pre-parental animals, when the adults were engaging in nestling provisioning. I recorded videos of white-throated sparrow nests to quantify nestling provisioning, among other parental behaviors. I focused on the nestling provisioning rate as the primary measurement of parental behavior, but I present data on other behaviors recorded from the videos in Table S5. I found that TS males provisioned their nestlings more often than did WS males (t = 2.059, p = 0.048; Figure 4A, Table S6), but I did not detect a similar morph difference in females (t = -1.154, p = 0.257; Figure 4A, Table S6).

I measured *VIP* expression using RT-qPCR to test for a morph difference in *VIP* expression in the IN. I did not detect a morph difference ($F_{(1,24)}$ = 0.079, p = 0.781; Figure 4B, Table S6), suggesting that any morph difference in *VIP* expression in this region, if it exists, is

not robust. However, I found a significant positive relationship between expression in this region and provisioning rate; when controlling for morph and sex in the model, I found that the higher the *VIP* expression in the IN, the more the individual fed its nestlings (R = 0.417, 95%CI [0.006, 0.708], p = 0.048; Figure 4C, Table S6). Notably, *VIP* expression in the AH was not significantly correlated with provisioning rate (R = -0.104, 95%CI [-0.512, 0.343], p = 0.655; Figure S3, Table S6), and the relationship between *VIP* expression and provisioning trended significantly stronger in the IN than in the AH (Fisher's Z: p = 0.091).

Because of the divergence between VIP^{2m} and VIP^{2} in *cis*-regulatory regions, I reasoned that differential expression of the alleles would contribute to the overall level of *VIP* expression within each brain region. To test for differential expression of the two alleles of *VIP*, I measured allelic imbalance in the IN of WS birds as described above. I found the same result in the IN as in the AH; VIP^{2m} was expressed more than VIP^{2} (one-sample t-test: t > 4.1, p < 0.5; Figure 5A, Table S7). I also found a non-significant, positive relationship between allelic imbalance and overall expression in the IN (R = 0.329, 95%CI [-0.220, 0.720], p = 0.231; Figure 5B; Table S7), which was similar in magnitude and direction to the correlation in the AH (Figure 3B). Next, I reasoned that because allelic imbalance predicted the overall expression of *VIP* in the IN and the overall expression of *VIP* in the IN predicted provisioning rates, then there should be a positive relationship between the provisioning rate and allelic imbalance in the IN. Indeed, I found a positive correlation that trended significant between the degree of allelic imbalance in the IN and provisioning rate (R = 0.534, 95%CI [-0.025, 0.838], p = 0.060; Figure 5C, Table S7). In contrast, there was no relationship between provisioning rate and allelic imbalance in the AH (R <0.001, 95%CI [-0.551, 0.551], p = 0.999; Figure S4, Table S7), but the degree of allelic imbalance in the IN was not more strongly correlated with provisioning than was the allelic

imbalance in the AH (Fisher's Z: $p = 0.183$).

Differential *VIP* expression depends on brain region

The aggressive and parental behavioral phenotypes of the WS and TS morphs are thought to represent the ends of a continuum between antagonistic life history strategies, sometimes referred to as a life history trade-off (Maney, 2008; Trivers, 1972). My findings demonstrated that *VIP* expression in the AH and IN is associated with aggression and parental care, respectively. *VIP* expression in the AH was higher in WS birds, which engage in an aggressive life history strategy, than in TS birds. In contrast, *VIP* expression in the IN appeared to be more similar between the morphs. This result suggests that the degree to which the morphs differ in *VIP* expression, and perhaps even the direction of that difference, might depend on the region of the brain. This result would be consistent with distinct behavioral roles for *VIP* expression in the AH and IN. To test for a statistical interaction between morph and brain region, which would show that the morph difference in VIP does depend on regions, I pooled data on *VIP* expression from the two cohorts, which increased statistical power, and conducted a MANOVA. I found a significant interaction between morph and brain region ($F_{(1,45)} = 12.16$, $p = 0.002$; Figure 6, Table S8), and in *post-hoc* tests for morph differences in expression within each brain region, I detected a morph difference in the IN ($t = 2.145$, $p = 0.037$) in a direction opposite from the morph difference in the AH ($t = -2.915$, $p = 0.005$; Figure 6, Table S8). In other words, when considering all the birds in the study together, *VIP* expression was *higher* in WS birds than TS birds in the AH but *lower* in the IN. This result differed from the result in the parental cohort, in which I did not detect a morph difference in IN, so I examined whether the morph difference in the IN seen after pooling the cohorts may have been due to a large difference in the IN of pre-parental animals only. Using MANOVA, I found that, like in the parental cohort, the main effect

of morph was not significant in the pre-parental cohort ($F_{(1,24)} = 1.175$, $p = 0.289$); however, the effect size was larger (pre-parental $\eta^2 = 0.05$; parental $\eta^2 < 0.01$). Furthermore, I found a morph difference in *VIP* expression in the IN in females in the pre-parental cohort ($t = 2.412$, $p = 0.024$) but not in males ($t = -0.744$, $p = 0.464$).

Because the aggressive and parental phenotypes in these sparrows are thought to represent the two ends of a life history trade-off, we might expect a negative relationship between territorial singing and parenting behavior. In fact, negative relationships between aggressive and parental behaviors have been repeatedly demonstrated in many species of vertebrates (Cunha et al., 2019; Ketterson & Nolan, 1994; Trivers, 1972). In this study, I measured aggressive or parental behavior, but not both in the same animals. I did, however, measure *VIP* expression in the AH and IN of all animals; therefore, I could test for a negative relationship between *VIP* expression in the AH and the IN. Indeed, *VIP* expression in the AH was negatively correlated with *VIP* expression in the IN: birds with high levels of *VIP* expression in the AH had low levels of *VIP* expression in the IN, and vice versa ($R = -0.318$, 95%CI [-0.542, -0.052], $p = 0.020$; Figure 7). This negative relationship suggests that there could be oppositional regulation of *VIP* expression in the AH and IN, which might be facilitated by an upstream factor that mediates the trade-off between aggressive and parental behaviors.

My results thus far illustrate that differential regulation of *VIP* expression between the morphs depends on brain region and may play a key role in the differences in behavior between WS and TS birds. Given that the *cis*-regulatory region of VIP^{2m} has diverged from VIP^{2} (Sun et al., 2018; Prichard et al., 2022), I reasoned that allele-specific expression, evidenced by allelic imbalance (Figures 3 & 5), could be a contributing factor to the morph differences in *VIP* expression within these two brain regions. However, I found that the allelic imbalance in the AH

and IN was in the same direction, with VIP^{2m} overexpressed relative to VIP^{2}, even though the morph differences in these two regions went in opposite directions. I thus inferred that if the direction of allelic imbalance does not differ between the AH and IN, then the degree of allelic imbalance might. To test this prediction, I pooled the cohorts and compared the degree of allelic imbalance between the two regions. I found that the degree to which VIP^{2m} was overexpressed, relative to VIP^{2}, was significantly greater in the AH than in the IN ($F_{(1,34)} = 4.604$, $p = 0.039$; Figure 8, Table S8).

The correlation between allelic imbalance and overall expression affected my interpretation of the results of the allelic imbalance assay. The results within each cohort suggested positive relationships between allelic imbalance and overall expression in both brain regions, but these correlations were not statistically significant in the AH (Figure 3B) or the IN (Figure 5B). Because I could detect a morph difference in *VIP* expression in the IN only after pooling the cohorts, I next tested for statistically significant relationships between allelic imbalance and overall expression in the pooled cohorts. I found a positive relationship that trended significant in the AH ($R = 0.367$, 95%CI [-0.015, 0.656], $p = 0.060$; Figure 9, Table S4). This finding was consistent with the correlations between allelic imbalance and overall expression within the parental cohort ($R = 0.427$, 95%CI [-0.134, 0.781], $p = 0.128$; Figure S5, Table S4) as well as within the pre-parental cohort (Figure 3B, Table S4). Together, these findings suggest a generally positive relationship between *VIP* expression and allelic imbalance in the AH. In the IN, however, in the pooled cohorts the degree of allelic imbalance negatively predicted the overall expression of *VIP* ($R = -0.447$, 95%CI [-0.663, -0.070], $p = 0.009$; Figure 10; Table S7). Within the pre-parental cohort, this correlation was also significant and negative ($R = -0.651$, 95%CI [-0.858, -0.235], $p = 0.005$, Figure S6, Table S7). Furthermore, the

correlation coefficient in the pre-parental cohort differed significantly from that in the parental cohort (Fisher's Z: $p = 0.005$) In other words, in the IN of animals that comprised the pre-parental cohort, the more that VIP^{2m} was expressed relative to VIP^{2}, the lower the total amount of *VIP* expression, and this relationship was reversed in the parental cohort.

Discussion

The two morphs of white-throated sparrows are a good example of alternative behavioral phenotypes (Maney, 2008; Tuttle, 2003). The behavioral phenotype of the WS morph represents an aggressive life history strategy, while the TS morph is less aggressive, in contrast (Kopachena & Falls, 1993a; Horton et al., 2014b). Existing evidence from other species suggests that *VIP* expression in the AH is associated with, and likely causal for, aggressive behavior in songbirds (Goodson et al., 2012a, b), and thus morph differences in *VIP* expression in this region may contribute to morph differences in aggression in white-throated sparrows (Horton et al., 2020a). The present study replicated the findings from a previous study showing that *VIP* expression in the AH is higher in WS birds than in TS birds during the breeding season and that *VIP* expression in this region predicts territorial singing independently of morph (Horton et al., 2020a). I expanded on these results by providing evidence of over-expression of the VIP^{2m} allele in the AH, which may underlie the morph difference in *VIP* expression in the AH and thus may contribute to downstream morph differences in aggression. The degree of allelic imbalance positively predicted both the overall expression of *VIP* and aggression. This differential expression of the *VIP* alleles may be due to divergence between the alleles in *cis*-regulatory elements (Prichard et al., 2020; Sun et al., 2018).

The aggressive life history strategy of the WS morph complements the parental life history strategy of the TS morph; TS birds tend to engage in parental care behavior, such as

provisioning nestlings, more than WS birds (Kopachena & Falls, 1993b; Knapton & Falls, 1982). In this study, I found that provisioning rates were higher in TS males than WS males, but I did not detect a morph difference in females. These results are consistent with some previous studies in which the morph difference in provisioning rate was detected in males but not in females (e.g., Horton & Holberton, 2010; Horton et al., 2014b, Horton et al., 2020a). As demonstrated by research conducted mainly in poultry and pigeons, VIP released by neurons in the IN regulates prolactin secretion from the anterior pituitary (reviewed by Kingsbury, 2015 and Smiley, 2019). Levels of *VIP* mRNA and VIP protein in the IN, as well as prolactin hormone in plasma, are correlated across reproductive stages in turkeys (Chaiseha et al., 1998). Thus, I hypothesized that morph differences in parental behavior may be mediated by morph differences in *VIP* expression in the IN. In a previous study, Horton et al. (2020a) used *in situ* hybridization to measure *VIP* expression in the IN of white-throated sparrows. In that study, they detected a morph difference in *VIP* expression in the IN of males but not females. They did not detect a relationship between *VIP* expression and provisioning rate. In contrast with those findings, in the present study *VIP* expression in the IN was greater in TS than WS birds in both sexes and both overall *VIP* expression and the degree of over-expression of VIP^{2m} in the IN predicted parental provisioning rate. These discrepancies between the results of these two studies may be due to differences in statistical power (see Limitations). Altogether, the results of these studies support the hypothesis that higher *VIP* expression in the IN of TS birds, which is expected to promote parental behavior via the presumed increase in VIP availability and thus have a potential positive impact on prolactin secretion, may contribute to the morph difference in nestling provisioning.

In this study, I provided evidence consistent with the hypothesis that the expression of a single gene, *VIP*, plays multiple roles in the behaviors that characterize the behavioral

polymorphism in white-throated sparrows. My findings that the morph difference in *VIP* expression in the AH went in a direction opposite from the morph difference in the IN, and that expression in the two regions was anticorrelated, suggest potentially common upstream regulation of *VIP* expression in these two disparate regions. Kingsbury & Wilson (2016) proposed that in songbirds, *VIP* expressed in the AH and IN play critical roles in mediating a trade-off between aggressive and parental behavioral phenotypes. In particular support of this hypothesis was a study in zebra finches (*Taeniopygia guttata*) demonstrating that parental behavior, measured as time spent in the nest, was correlated positively with *VIP* expression, measured with *in situ* hybridization, in the IN but negatively in the AH (Kingsbury et al., 2015). The results of the present study demonstrated slightly different relationships between parental behavior and *VIP* expression measured by qPCR; nestling provisioning correlated positively with *VIP* expression in the IN, but it did not correlate with *VIP* expression in the AH. In addition, I showed that territorial singing correlated positively with *VIP* expression in the AH, but did not correlate with *VIP* expression in the IN. These results suggest that *VIP* expression in neither the AH nor the IN directly mediates a trade-off between aggression and parental care. However, the finding that *VIP* expression in these two regions is negatively correlated supports the hypothesis that *VIP* could represent the target of a single, upstream mediator of both aggression and parental care. By responding to this signal differently in the AH and IN, VIP may modulate both behaviors in a way that subserves the life history strategy that is most adaptive for each morph.

Gene regulatory networks represent the coordinated expression of many genes, often in response to social and environmental stimuli (Sinha et al., 2020). Likewise, supergenes are hypothesized to link genes that function together to orchestrate complex phenotypes (Charlesworth, 2016; Schwander et al., 2014; Thompson & Jiggins, 2014); thus, we may find

candidates for an upstream element that regulates *VIP* expression either within the supergene or within a gene regulatory network affected by the supergene. Previous work from our lab has focused, for example, on steroid-related genes inside the supergene. These genes are interesting candidates in part because plasma levels of circulating steroid hormones, such as testosterone and estradiol, exhibit robust morph differences in white-throated sparrows (e.g., Horton et al., 2014b; Spinney et al., 2006). Unlike VIP and prolactin, however, steroid hormones are not encoded by individual genes. Instead, multiple genes, including those that encode enzymes and receptors, regulate steroid levels, and mediate their effects (Lipshutz et al., 2019). Morph differences in mRNA expression for steroidogenic enzymes and steroid receptors have been reported in several regions of the social behavior network in the brain (Grogan et al., 2019; Horton et al., 2014a). Of particular note is *ESR1* (e.g., Merritt et al., 2020; reviewed by Maney et al., 2020), which is separated from *VIP* by just one gene within the supergene (Maney et al., 2020). It could be that a steroid hormone like testosterone or estradiol mediates morph differences in *VIP* expression via the action of steroid receptors.

Steroids and their receptors represent an especially compelling candidate for an upstream regulator of *VIP* expression because they have been proposed to mediate a trade-off between aggressive and parental behavioral phenotypes in vertebrates (Hau, 2007), and a large body of research supports this hypothesis (Wingfield et al., 1990; Ketterson & Nolan, 1994). Circulating prolactin and steroid hormones are elevated in breeding compared with non-breeding birds; however, their secretion is typically out of phase throughout the breeding season such that circulating levels of steroid hormones decrease as circulating levels of prolactin increase and vice versa (Massaro et al., 2007; Seiler et al., 1992; Wingfield & Goldsmith, 1990). This negative association between pro-aggression and pro-parenting endocrine states may reflect the

trade-off between aggressive and parental behavioral states (Ketterson & Nolan, 1994; Lynn, 2016; Van Roo, 2003; but see Valdez, 2022).

Steroids could regulate *VIP* expression directly via putative consensus sequences for androgen receptor (AR) and ERα in the *VIP* promoter (Prichard, TRANSFAC database, unpublished observation). Polymorphisms in these consensus sequences could thus cause allele-specific expression of VIP^{2m}; for instance, a SNP has resulted in an additional putative AR consensus sequence on VIP^{2m} that is not on VIP^{2} (Prichard, TRANSFAC database, unpublished observation). *VIP* expression may also be affected by the non-genomic effects of estradiol; *VIP* expression is dependent on a cAMP-responsive element (Hahm & Eiden, 1996, 1998), and estradiol can affect cAMP signaling via membrane-bound estrogen receptors (Balthazart & Ball, 2006; Heimovics et al., 2018). Currently, it is unknown whether *VIP* expression in the brain responds to changes in steroid hormones in white-throated sparrows. In brain regions other than the AH and IN, and in other species of birds, *VIP* expression appears to be sensitive to increases in testosterone (*Coturnix japonica*, Aste et al., 1997) and decreases in aromatase (*Melospiza melodia*, Wacker et al., 2008). In rats, treatment with exogenous estradiol stimulated VIP release from the mediobasal hypothalamus (Lasaga et al., 1991) as well as *VIP* expression from the anterior pituitary (Montagne et al., 1995). These examples demonstrate that, at least in some brain regions and some model organisms, *VIP* expression appears to be sensitive to changes in steroid hormone levels.

Steroid receptor-mediated *VIP* expression is particularly noteworthy because morph differences in *VIP* expression could be driven by morph differences in circulating steroid hormone levels (e.g., Horton et al., 2014b), steroidogenic enzymes, or steroid receptors (e.g., Grogan et al., 2019; Horton et al., 2014a). Using RT-qPCR, Grogan et al. (2019) measured the

expression of steroid-related genes in the hypothalamus of free-living white-throated sparrows. They found that AR and aromatase mRNA were expressed more in the hypothalamus of WS birds than TS birds (Grogan et al., 2019). They also found a trend for a morph difference in ERα expression in the same direction (Grogan et al., 2019; c.f. Horton et al., 2014a). Thus, if testosterone regulates *VIP* expression via androgen receptors, for example, then my result that WS birds have higher *VIP* expression in the AH than TS birds could be explained by one or more of the following: increased levels of circulating testosterone in WS birds, increased expression of androgen receptor in WS birds, and increased expression of VIP^{2m} via an additional putative consensus sequence for androgen receptor on that allele. Similarly, morph differences in circulating estradiol, aromatase expression, or expression of ERα could also explain my result in the AH.

My findings demonstrate that the regulation of *VIP* expression differs between the AH and IN in a behaviorally relevant way; the morph difference in *VIP* expression in the IN went in a direction opposite from the morph difference in the AH. Thus, if steroids and the expression of steroid-related genes are driving the morph differences in the AH as well as the IN, then those mechanisms must be functioning differently within each of the two regions. It is reasonable to expect that the level of steroids arriving from the circulation would be similar between brain regions, but the expression of steroid-related genes (i.e., receptors, enzymes, etc.) may vary. Only a few existing studies have begun to address the question of whether morph differences in steroid-related gene expression may depend on brain region, specifically the AH and IN, but they also present challenges in this context. Grogan et al. (2019) measured the expression of steroid-related genes in a sample of the hypothalamus that included the AH, in addition to other nuclei, but likely missed the IN. The heterogeneity of the samples may have prevented detection of

morph differences in the expression of steroid-related genes in the AH and IN specifically.

The issue of heterogeneity is relevant in another study in which RNA-sequencing was used to explore patterns of gene expression in the hypothalamus of white-throated sparrows (Zinzow-Kramer et al., 2015). In that study, expression of *VIP* did not correlate with that of steroid-related genes in a weighted gene co-expression network analysis. However, in a different passerine species, the wire-tailed manakin (*Pipra filicauda*), *VIP* was co-expressed with steroid-related genes in samples of the hypothalamus that contained the ventromedial hypothalamus and medial preoptic area (Horton et al., 2020b). In that study, these relationships were not reported for the AH or IN, specifically. Together, these findings and the results of the present study highlight the value of and need for research in which gene expression is measured in multiple precisely identified brain regions.

Another candidate for an upstream regulatory factor that might modulate *VIP* expression is dopamine. The dopamine receptor 2 (D2) agonist bromocriptine is commonly used to experimentally suppress prolactin levels and consequently affect parental behavior across vertebrates, including birds (reviewed by Smiley, 2019; Angelier et al., 2006; Ruiz-Raya et al., 2021; Smiley & Adkins-Regan, 2018; Thierry et al., 2013), mammals (Bridges & Ronsheim, 1990; Chen et al., 2023; Roberts et al., 2001), and fish (Cunha et al., 2019; Kindler et al., 1991). In turkeys, the genes encoding dopamine receptor 1 (*DRD1*) and dopamine receptor 2 (*DRD2*) are co-expressed with *VIP* in neurons of the IN and exert stimulatory and inhibitory effects on VIP expression, respectively (reviewed by Smiley, 2019). In turkeys, for example, infusion of dopamine into the third ventricle increased *VIP* expression the IN (Bhatt et al., 2003). Dopamine receptors have also found to exert effects on VIP release, in hypothalamic explants from turkeys, perifusion of a dopamine receptor 1 (D1) antagonist blocked VIP release, whereas D1 agonist

and D2 antagonist both stimulated VIP release (Chaiseha et al., 1997). The precise mechanism by which D1/D2 receptor binding to neurons of the IN may affect *VIP* expression is yet to be determined. However, as previously mentioned, a cAMP-responsive element in the *VIP* promoter is critical for *VIP* expression *in vitro* (Hahm & Eiden, 1996, 1998), and D1 binding promotes whereas D2 binding interferes with cAMP signaling (Trantham-Davison et al., 2004). Therefore, differential allele-specific expression of *VIP* expression, as evidenced by allelic imbalance in this study, could result from a genetic polymorphism in a cAMP-response element.

It is currently unknown whether *DRD1/DRD2* expression differs between the morphs in the AH and IN of white-throated sparrows. Chaiseha et al. (2003) used *in situ* hybridization to measure both *DRD1* and *DRD2* receptor expression in a variety of brain regions in turkey hens across multiple stages of the reproductive cycle. They demonstrated that *DRD2* expression did not change between non-breeding and breeding conditions in any region they examined, whereas *DRD1* expression increased in most of the regions. The degree of this increase varied, however, between the AH and the IN: *DRD1* expression appeared to increase more in the AH than in the IN between the non-breeding and breeding conditions (Chaiseha et al., 2003). Importantly, because D1 has a lower binding affinity for dopamine than D2 (Richfield et al., 1989), the response of a target cell to dopamine depends on the abundance of D1 relative to D2 in that cell (Hunger et al., 2020). Thus, to put the results from Chaiseha et al. (2003) in another way, the relative expression of *DRD1* to *DRD2* was higher in the AH than the IN of turkeys in breeding condition, which may result in a stronger inhibitory effect of D2 binding in the IN than in the AH.

If these findings in turkeys are generalizable to white-throated sparrows, they could explain my result of a negative relationship between the degree of allelic imbalance and overall

VIP expression in the IN of pre-parental animals. This relationship contrasted with that in the AH, in which the relationships between the degree that VIP^{2m} was overexpressed and level of overall expression were strictly positive in both pre-parental and parental animals. The difference in the relative expression of *DRD1/DRD2* in the AH and IN demonstrated by Chaiseha et al. (2003) could explain the negative relationship between allelic imbalance and overall expression in the IN of WS birds if, for example, the VIP^{2} allele is more strongly affected by the inhibitory effect of D2 receptor binding than VIP^{2m} due to genetic polymorphisms. In that case, overall expression of *VIP* would decrease as VIP^{2} expression is downregulated relative to VIP^{2m}, which would be evidenced by increased allelic imbalance. On the other hand, the inhibitory effect of D2 receptor binding may be less pronounced in the AH, where *DRD1* expression increased more than in the IN at the onset of breeding condition (Chaiseha et al., 2003).

Determining the precise regulatory factors that affect *VIP* expression in the AH and IN is a question beyond the scope of the present study. That said, this study provides important information about the contexts in which *VIP* expression is regulated differently between the morphs and between the ZAL2 and $ZAL2^{m}$ alleles, which may shed light on the position of this critical gene within a gene regulatory network that orchestrates trade-offs between aggression and parental care. This research highlights the importance of a hypothesis-driven, bottom-up approach to understanding the molecular and genetic underpinnings of complex phenotypes and life history trade-offs.

Limitations and future directions

In this study, *VIP* expression in the IN was greater in TS than WS birds in a sample that included two cohorts of animals, one collected early and one late in the breeding season. I did not, however, detect this morph difference when I considered each of these sampling cohorts

separately. I believe my inability to detect the morph difference in the IN within each cohort was most likely an issue of statistical power and sampling method. In a previous study, we demonstrated a morph difference in *VIP* expression in the IN of male white-throated sparrows engaged in nestling provisioning (Horton et al., 2020a). Because we used in situ hybridization in that study to measure expression precisely within the boundaries of IN, we had greater neuroanatomical precision than is possible with the microdissection punch method used in the present study. Thus, the data presented here may have been noisier, and therefore the morph differences may have been more difficult to detect. It is interesting that Horton and colleagues (2020a) did not detect a relationship between *VIP* expression and nestling provisioning, whereas I detected a significant positive relationship. Thus, although. both the previous study and the present study had a null finding, together they tell similar stories.

It is worth noting that there may be a ceiling effect on VIP-mediated prolactin secretion. That is, prolactin secretion stimulated by VIP may be at a maximum in animals already engaged in offspring care (Christensen & Vleck, 2008, as cited by Smiley, 2019). This ceiling effect could explain relatively small effect sizes for morph differences in parental behavior and *VIP* expression. My finding that the main effect of morph on *VIP* expression in the IN of animals in the pre-parental cohort was larger than in the parental cohort is consistent with this perspective. Although the animals in the pre-parental cohort were not engaging in nestling care, which is the most demanding form of parental investment in species with altricial offspring (Goldsmith, 1982), females in this study, in particular, were engaged in other parental behaviors, like nest-building, egg laying, and occasionally incubating (Prichard, personal observation). Thus, the morph difference in *VIP* expression in the IN of pre-parental animals suggests that there may also be morph differences in these early-season parental behaviors. In future studies, it may be

worth quantifying forms of parental investment during both early breeding and nestling stages.

The issue of low statistical power may have also been at play in my inability to detect statistically significant relationships between allelic imbalance and overall expression. In the AH, the correlation was positive and trending significant after pooling the two cohorts ($p = 0.06$), but within each cohort, these relationships were not statistically significant ($p > 0.10$). Notably, the effect sizes and directions of this relationship within all subsets of data are similar. In the parental cohort, the correlation between allelic imbalance and overall expression in the IN was also positive but not significant. As was the case for the AH, I suspect this relationship is positive and repeatable but not well-powered in my sample. However, in contrast to the results from the AH, the relationship between overexpression of VIP^{2m} relative to VIP^{2} and overall expression in the IN was significantly negative after pooling the two cohorts, and this result appeared to be driven by a strong, negative correlation in the pre-parental cohort. The negative and positive relationships in the pre-parental and parental cohorts, respectively, suggest that the regulation of *VIP* expression in the IN may change over time, perhaps due to changes in breeding condition or social/environmental stimuli, which may be a good future direction of research.

Conclusion

This study demonstrated that the way *VIP* expression is regulated—which depends on plumage morph, allele, and brain region—may be critical for optimizing life history strategies. My results are consistent with existing evidence that *VIP* expression in the AH plays a positive role in aggression, and that *VIP* expression in the IN plays a positive role in parental care. I found that although *VIP* expression in both the AH and IN differed by morph, the differences went in opposite directions: In the AH, *VIP* was expressed more in the WS birds than TS birds, whereas in the IN, the TS birds had higher expression. By quantifying allelic imbalance, I

demonstrated that VIP^{2m} is overexpressed relative to VIP^{2} to a significantly greater extent in the AH than in the IN. These results suggest that *VIP* may respond to upstream regulatory factors in a brain region-dependent manner. I propose that AR, ESR1, and DRD1/DRD2 receptors are strong candidates for upstream factors that may regulate *VIP* expression in these two regions in a behaviorally relevant way. Once one or more of these upstream regulatory factors establish morph differences in *VIP* expression, brain region-specific downstream effects of VIP may maximize the behavior most beneficial to each morph's life history strategy by promoting either aggression or parental care. Overall, this study demonstrated that a single pleiotropic gene may contribute to the expression of alternative behavioral phenotypes in a polymorphic species through its role in multiple aspects of a behavioral polymorphism, and it provides direction for future research on how genes within a supergene interact to affect complex phenotypes.

Methods

Study Population

All sparrows were collected from an 18,000 acre property owned by Boulder Lake Environmental Learning Center near Duluth, Minnesota, U.S.A., during May – July of 2019 and 2021. All research was carried out with the approval of the Emory University Institutional Animal Care and Use Committee and with appropriate local (St. Louis County Land and Minerals Department, Authorization Number A1021002), state (Minnesota Department of Natural Resources, Special Permits 23705 and 30224), and federal (U.S. Geological Survey, USGS Permit Number 23369; U.S. Fish and Wildlife Service permit number MB009702-0) permits.

Behavior

The individuals in this study comprised two cohorts, referred to here as pre-parental and

parental. Territorial behavior was quantified for the pre-parental cohort during the early breeding season, before the start of incubation, and parental behavior was quantified for the parental cohort later in the breeding season when adults were engaged in nestling provisioning, and all breeding pairs were heteromorphic (i.e., one TS and one WS adult, for sample sizes refer to Table S1). The birds in the two cohorts were collected from different parts of the property to minimize disturbances and cross-exposure to stimuli (e.g., exposure of parental animals to decoys, see Territorial Behavior, below). Birds were captured for banding an average of 16 days before the first behavioral observation, except for two birds in the parental cohort that were not banded.

All birds were trapped by luring them into mist nets with playback of conspecific song. All birds were fitted with an aluminum USGS identification band and plastic bands in a unique color combination for identification during behavioral observations. Morphological measurements, including mass, total head length, wing cord, and tarsus length, were taken at this time. In addition, we evaluated the breeding stage for each animal in hand by measuring the width and height of the cloacal protuberance for males and scoring the development of the brood patch for females. All birds were released at the site of capture. We continuously monitored all breeding pairs throughout the breeding season and noted their progression through the breeding stages by observing nesting behaviors such as nest building, incubation, or nestling provisioning. Data collection from the pre-parental cohort ceased once it was determined that most of the females were laying eggs and beginning to incubate. At this point in time, our efforts shifted to nest searching. Data collection or the parental cohort began once the nestlings were 4-days post-hatch and continued until the end of the summer.

Pre-parental Cohort

Studies on territorial aggression were conducted during early summer (May 14 – Jun 5, 2019; May 16 – Jun 3, 2021). We determined the boundaries of the territories of breeding pairs based on behavioral observations of the focal pair and neighboring pairs. Territorial aggression was quantified using simulated territorial intrusions (STIs). A caged, male conspecific decoy, captured at least 4.5 miles from the site of the STI, was placed within the territory of a focal pair along with a Bluetooth speaker (model: FBA_AYL-SoundFit) playing conspecific song. All STIs were conducted in the morning (0530-1130 EDT). STIs were performed twice, once on two consecutive days, to present each breeding pair with a male decoy of each morph separately, and which morph was presented on the first day was balanced across trials (Horton et al., 2012). Each decoy was paired with a unique playback recording from the same library used by Horton et al. (2014b) and presented only four times: once first and once second for each of the two pair types (WSM/TSF, WSF/TSM). Decoys were released near the location of capture.

The STI protocol and the behaviors recorded were as previously described by Horton et al. (2014b). Two observers with unique viewpoints of the decoy and focal bird(s) performed the STIs. After placing the caged decoy and speaker, one of the observers began playback, and each began their own timer and recorded their observations. If neither member of the focal pair appeared within 15 minutes, the trial was stopped and we returned the next day to try again in a different part of their territory, when possible. Otherwise, when the first member of the focal pair showed interest in the decoy, the observers began a 10-minute countdown. During the following 10-minute period, the observers recorded territorial behavior from each bird in the focal pair. The behaviors that were recorded included singing, time of first approach, time spent within 5 m of the decoy, time spent within 2 m of the decoy, distance of the closest approach and any physical

contact with the cage, flights over/toward the cage, other vocalizations (e.g., chips, chip-ups, trills), and copulation solicitations (see Table S2 for more detailed descriptions of the behaviors). At the end of the 10-minute STI, the two observers compared their observations and agreed on the final data set for each trial. Discrepancies were resolved either by using the data from the observer with a better line of sight or by using the average.

Parental Cohort

Parental behavior was quantified in the parental cohort during mid-summer (June 15 – July 16, 2019 and June 9 – July 10, 2021) when adults were engaged in nestling provisioning. Video recordings of parental behavior were collected when nestlings at the recorded nest were 5-7 days post-hatch. Nestling age was typically based on the known hatch date for the nest, but for nests that were found after hatching, the age of the nestlings was visually evaluated following U.S. Fish & Wildlife guidelines (Jongsomjit et al., 2007). All recordings were made between 0530 – 1200 EDT and during fair weather. Cameras (Sanyo Xacti MPEG-4 AVC/H.264) were placed 2 – 6 ft from the nest, depending on the cover provided by surrounding vegetation. The cameras were left to record for 2-3 hours.

Video recordings were stored on a hard drive until they were evaluated by one or two scorers who were blind to the hypotheses about morph differences. Agreement between scorers for the parental data was tested with the intraclass correlation coefficient (ICC) using icc (irr package, Gamer & Lemon, 2019; Koo & Li, 2016). Approximately 28% of the videos were scored by both scorers, and the data from this subset were highly consistent between the scorers (ICC = 0.980 ± 0.018). Behaviors that were quantified from the videos included nestling provisioning, fecal sac removals, brooding, and time spent at the nest (see Table S5 for more detailed descriptions of the behaviors). The video scorers attributed behavior to each adult parent

by observing band colors when possible or plumage coloration (WS or TS) when bands were not visible. Scorers also noted some behaviors that occurred off-camera (e.g., chipping vocalizations). All behavior scoring was conducted in BORIS (v. 7.13.9; Friard & Gamba, 2016).

Tissue Collection

Birds were captured for tissue collection 1-2 days after the second STI for the pre-parental cohort and on post-hatch day 7 or 8 for the parental cohort. Capture by mist net occurred 3.5 ± 5.3 min (mean ± SD; both cohorts combined) after the start of playback. Directly after capture (3.5 ± 1.5 min after capture), a blood sample was taken from the brachial vein (up to 300µl) using a 26-guage needle and heparinized capillary tubes. A second blood sample of up to 1ml was collected from the jugular vein (7.5 ± 3.5 min after capture) under deep isoflurane anesthesia immediately before decapitation. Blood samples were stored on ice for ~3 hours before centrifuging. Brains were dissected and flash-frozen on powdered dry ice at 11 ± 4 min after capture. Pituitary glands were removed and stored in RNALater (Invitrogen; Waltham, MA) at room temperature for at least two days before freezing. Gonads were flash-frozen on powdered dry ice for use in another study. The brain and gonads, in addition to a liver sample, were stored on dry ice for ~3 hours until transferred to a -80˚C freezer. The breeding stage was reassessed at this time based on the measurements of the cloacal protuberance, the development of the brood patch, and/or presence of eggs in the female's oviduct. When present, nestlings were also collected and euthanized by overdose of isoflurane at the same time as the adults and used for another study. The age of the nestlings was re-evaluated in hand upon collection (Jongsomjit et al., 2007). If our estimation of the age of the nestlings was adjusted at this stage, then the days post-hatch was corrected for all videos from that nest and the video from corrected day 6 post-

hatch was used for behavioral scoring. Brain, liver, gonad, and pituitary tissues from the adults were kept at -80˚C and plasma samples were kept at -20˚C until they were transported on dry ice to Emory University.

Microdissection and DNA/RNA extraction

Frozen brains were sectioned at 200µm thickness and thaw-mounted onto microscope slides. Regions containing the AH and IN were microdissected using the Palkovits punch technique (Palkovits, 1985). Punches 1 mm in diameter were bilateral when targeting the anterior hypothalamus and centered on the midline when targeting the infundibular nucleus of the hypothalamus (Figure S7). Punched tissues were preserved in DNA Shield (Zymo; Irvine, CA, USA) and frozen at -20˚C until RNA extraction. DNA/RNA extractions were conducted using the Quick DNA/RNA Microprep Kit (Zymo). Extracted DNA was stored for use in another study. Extracted RNA was quantified by Nanodrop and cDNA converted on the same day with the Transcriptor High Fidelity cDNA Synthesis Kit (Qiagen; Valencia, CA, USA). The cDNA conversions included two negative controls to test for gDNA contamination: a reaction without reverse transcriptase and a no template control.

VIP expression

Expression of the *VIP* gene was measured using RT-qPCR performed using a Roche LightCycler 480 Real-Time PCR System. Two housekeeping genes (HKGs), glyceraldehyde-3-phosphate dehydrogenase (*GAPDH*) and peptidylprolyl isomerase A (*PPIA*), were selected because their expression is stable across individuals and does not differ by morph in brain tissue in this species (Zinzow-Kramer et al., 2014). Primers and probes for *VIP* and HKGs were designed and manufactured by Integrated DNA Technologies (Coralville, Iowa, USA) to target a region that included an intron-exon boundary for each gene (Table S9). Primers were validated

with a cDNA template by visualizing PCR amplicons on an agarose gel to confirm specificity in both morphs. Each 10µl qPCR reaction contained 2.5µl of cDNA template diluted 1:10, 5µl of PrimeTime Gene Expression Master Mix (IDT), 1µl of gene-specific primers (10nM), 0.5µl gene-specific probe (5nM), and 1µl Dnase/Rnase free H_2O. Cycling conditions were 1 cycle at 95˚C for 3 minutes, 45 cycles at 95˚C for 5 seconds and 60˚C for 30 seconds, and 1 cycle at 37˚C for 1 minute. Morph and sex were balanced across each qPCR plate, and samples collected in different years were run on separate plates to group the nuisance variables of year and plate together. Each plate included both brain regions (AH and IN) for each individual as well as four inter-run calibrator samples and two negative controls to test for gDNA contamination during cDNA conversion: a negative reverse transcriptase control and a negative template control. The four inter-run calibrator samples were each a unique pool of cDNA extracted from brain tissue collected from the hippocampus at the same time as the punches for the AH and IN (Figure S8). A standard curve of cDNA with a 1:5 dilution factor was used to assess amplification efficiency. Cp values were calculated using the "Abs quant/Second derivative max" method in the LightCycler Program (software v. 1.5.0). All samples were run in triplicate; if the standard deviation of Cp for a triplicate was greater than 0.2 then one technical outlier was removed. If the standard deviation of the sample was still greater than 0.2 after removing a technical outlier, the sample was designated as hyper-variable and either re-run or excluded.

Calculating relative expression

Cp values were exported and subsequent analyses were conducted in R (R version 4.3.0) and Rstudio ("Mountain Hydrangea" Release, (583b465e, 2023-06-05) for Windows). The expression of *VIP* relative to HKGs was calculated on the basis of Hellemans et al. (2007), and all formulas are described in the Appendix. Briefly, Cp values were averaged across technical

replicates, and amplification efficiency was calculated from the linear slope of the standard curve (Appendix, Formula 1; gene-specific efficiency values: *VIP* = 2.033 ± 0.053; *GAPDH* = 2.068 ± 0.058; *PPIA* = 2.026 ± 0.055). The Cp for each sample was standardized to the mean of all samples for that gene/probe (Appendix, Formula 2). A linear relative quantity for each sample/gene was calculated using the amplification efficiency (Appendix, Formula 3) and the linear relative quantity of the gene of interest (*VIP*) was normalized to the geometric mean of the two HKGs (Appendix, Formula 4). Finally, the relative expression values were equalized across qPCR runs using a normalization factor based on the mean of the inter-run calibration samples.

VIP allelic imbalance

The degree of allelic imbalance in *VIP* expression was quantified using a multiplexed qPCR assay designed and manufactured by Integrated DNA Technologies (Coralville, Iowa, USA). Primers amplified a region of the 3'UTR containing a C/T SNP that was then targeted by allele-specific probes (Table S9). The probe targeting the ZAL2 allele was labeled with 6-FAM fluorescent dye and the probe targeting the ZAL2^{m} allele was labeled with 5Cy5 fluorescent dye. The difference in fluorescence between these two probes allows them to be distinguished in a duplex reaction without color compensation (LightCycler 480 Manual; Roche Diagnostics, Indianapolis, IN). Primers were validated using cDNA from both morphs by visualizing PCR amplicons on an agarose gel to confirm specificity. All samples were run in triplicate on the same plate, and technical outliers were excluded. Only heterozygous WS cDNA samples were used in this assay because TS birds are homozygous for the *VIP*^{2} allele and, therefore, do not exhibit allelic imbalance. qPCRs were performed in volumes of 10µl including 5µl of PrimeTime Gene Expression Master Mix (IDT), 1µl of forward and reverse primers (5nM), 0.25µl *VIP*^{2m}-specific probe (10nM), 0.25µl *VIP*^{2}-specific probe (10nM), and 1µl DNase/RNase

free H_2O. Cycling conditions were 1 cycle at 95˚C for 3 minutes, 45 cycles at 95˚C for 5 seconds and 60˚C for 30 seconds, and 1 cycle at 37˚C for 1 minute.

Each plate included a standard curve to confirm that the allele-specific probes had similar and satisfactory amplification of both alleles. This standard curve was made with a 1:5 dilution factor using gDNA samples from heterozygous individuals, which have a 1:1 ratio of the ZAL2:ZAL2^m alleles. This standard curve also provided the slope for the amplification efficiency used in subsequent calculations. To confirm that the specificity of the probes was similar across degrees of allelic imbalance, we used gDNA from a rare ZAL2^m/ZAL2^m homozygote (Horton et al., 2013) and a TS bird (i.e., a ZAL2/ZAL2 homozygote) to create a second standard curve of known ratios of ZAL2^m : ZAL2 gDNA along a linear scale (1:8, 1:4, 1:2, 1:1, 2:1, 4:1, 8:1). The Cps measured from this second standard curve were converted into ratios (ZAL2^m : ZAL2) and plotted against the expected ratio to test for a linear relationship (Figure S8). In addition to these two standard curves, a sample of gDNA from the ZAL2^m/ZAL2^m homozygote and a TS bird were included on each plate to confirm minimal amplification of the ZAL2 allele in the ZAL2^m sample and vice versa. Two negative controls, a negative cDNA reverse transcriptase control and a negative RNA template control, were also included to test for gDNA contamination in the cDNA conversion. Lastly, tissue collected from the hippocampus at the same time as the punches for the AH and IN (Figure S7) was used to create four unique cDNA pools, samples of which were included on all plates to adjust for variation between runs.

Calculating allelic imbalance

Cp values were calculated using “Abs quant/Second derivative max” in the LightCycler Program (software v. 1.5.0). The relative expression of each allele, that is, VIP^{2m} / VIP^{2}, was

calculated for both the AH and IN for each bird based on methods described by Hellemans et al. (2007) and Merritt et al. (2020). All formulas are presented in the Appendix. Briefly, the mathematical protocol for this assay was the same as in the relative expression qPCR assay, described above, but instead of *VIP*:(*GAPDH*, *PPIA*), the relative expression quantified was VIP^{2m}:VIP^{2} (see Appendix, Formula 4, Examples 1 and 2). Because the primers for this assay were not intron-spanning, gDNA contamination was a concern. Therefore, I tested all samples for gDNA contamination using an intronic qPCR assay. gDNA contamination was calculated as the concentration of intronic signal divided by the concentration of the allele-specific signal. gDNA contamination was minimal for all samples (< 0.007), and no samples were excluded because of gDNA contamination.

Statistical Analyses

Statistical analyses were conducted in R (R version 4.3.0) and RStudio ("Mountain Hydrangea" Release, (583b465e, 2023-06-05) for Windows). All data on aggressive behavior were $\log_{10}$ transformed, and all data for parental behavior were square-root transformed for all statistical analyses. Data on *VIP* expression were $\log_2$ transformed. For all statistical models that included it, date was defined as the number of days since the last snowfall for each year (e.g., last snowfall on 5/1/19 and data collected on 5/10/19 = 9 days). Skewness/normality of each variable was tested with shapiro.test (stats package; R Core Team). Outliers were identified using grubbs.test (outliers package; Komsta, 2022) and excluded from downstream analyses. I took a two-step approach to test for differences between groups, starting with an ANOVA model that included relevant covariates and interactions and following up with within-group *post-hoc* Tukey HSD tests when appropriate. For example, if I found a significant interaction between morph and sex when testing for a morph difference with ANOVA, then I tested for and reported morph

differences within sex based on *post-hoc* Tukey HSD. MANOVAs and MANCOVAs were conducted with lme (nlme package; Pinheiro, et al., 2023; Pinheiro & Bates, 2000). *Post-hoc* Tukey HSD tests were conducted with emmeans (emmeans package; Lenth, 2023). Partial Pearson's correlations were conducted by calculating residual values by fitting the data to a linear model controlling for relevant covariates using lme (nlme package) and then testing for correlations with cor.test (stats package; R Core Team). I used Fisher's Z to test for differences between correlations. I tested for evidence of allelic imbalance using one-sample student's t-tests (t.test, stats package; R Core Team). All figures were created using the ggplot2 package (Wickham, 2016).

References

Angelier, F., Barbraud, C., Lormée, H., Prud'homme, F., & Chastel, O. (2006). Kidnapping of chicks in emperor penguins: A hormonal by-product? *Journal of Experimental Biology*, *209*(8), 1413–1420. https://doi.org/10.1242/jeb.02138

Aristizabal, M. J., Anreiter, I., Halldorsdottir, T., Odgers, C. L., McDade, T. W., Goldenberg, A., Mostafavi, S., Kobor, M. S., Binder, E. B., Sokolowski, M. B., & O'Donnell, K. J. (2020). Biological embedding of experience: A primer on epigenetics. *Proceedings of the National Academy of Sciences*, *117*(38), 23261–23269. https://doi.org/10.1073/pnas.1820838116

Aste, N., Viglietti-Panzica, C., Balthazart, J., & Panzica, G. (1997). Testosterone modulation of peptidergic pathways in the septo-preoptic region of male Japanese quail. *Avian and Poultry Biology Reviews*, *8*, 77–93.

Ball, G. F., & Balthazart, J. (2004). Hormonal regulation of brain circuits mediating male sexual behavior in birds. *Physiology & Behavior*, *83*(2), 329–346. https://doi.org/10.1016/j.physbeh.2004.08.020

Balthazart, J., & Ball, G. F. (2006). Is brain estradiol a hormone or a neurotransmitter? *Trends in Neurosciences*, *29*(5), 241–249. https://doi.org/10.1016/j.tins.2006.03.004

Barcelo-Serra, M., Gordo, O., Gonser, R. A., & Tuttle, E. M. (2020). Behavioural polymorphism in wintering white-throated sparrows, *Zonotrichia albicollis*. *Animal Behaviour*, *164*, 91–98. https://doi.org/10.1016/j.anbehav.2020.04.002

Bentz, A. B., George, E. M., Wolf, S. E., Rusch, D. B., Podicheti, R., Buechlein, A., Nephew, K. P., & Rosvall, K. A. (2021). Experimental competition induces immediate and lasting effects on the neurogenome in free-living female birds. *Proceedings of the National Academy of Sciences*, *118*(13). https://doi.org/10.1073/pnas.2016154118

Bhatt, R., Youngren, O., Kang, S., & Halawani, M. E. (2003). Dopamine infusion into the third ventricle increases gene expression of hypothalamic vasoactive intestinal peptide and pituitary prolactin and luteinizing hormone b subunit in the turkey. *General and Comparative Endocrinology*, *130*, 41–47.

Bole-Feysot, C., Goffin, V., Edery, M., Binart, N., & Kelly, P. A. (1998). Prolactin (PRL) and its receptor: Actions, signal transduction pathways and phenotypes observed in PRL receptor knockout mice. *Endocrine Reviews*, *19*(3), 225–268. https://doi.org/10.1210/er.19.3.225

Bridges, R. S., & Ronsheim, P. M. (1990). Prolactin (PRL) Regulation of maternal behavior in rats: Bromocriptine treatment delays and PRL promotes the rapid onset of behavior. *Endocrinology*, *126*(2), 837–848. https://doi.org/10.1210/endo-126-2-837

Campagna, L. (2016). Supergenes: The genomic architecture of a bird with four sexes. *Current Biology*, *26*(3), R105–R107. https://doi.org/10.1016/j.cub.2015.12.005

Chaiseha, Y., Youngren, O., Al-Zailaie, K., & El Halawani, M. (2003). Expression of D1 and D2 dopamine receptors in the hypothalamus and pituitary during the turkey reproductive cycle: Colocalization with vasoactive intestinal peptide. *Neuroendocrinology*, *77*(2), 105–118. https://doi.org/10.1159/000068649

Chaiseha, Y., Youngren, O. M., & El Halawani, M. E. (1997). Dopamine receptors influence vasoactive intestinal peptide release from turkey hypothalamic explants. *Neuroendocrinology*, *65*(6), 423–429. https://doi.org/10.1159/000127205

Chaiseha, Y., Youngren, O. M., & El Halawani, M. E. (1998). Vasoactive intestinal peptide secretion by turkey hypothalamic explants. *Biology of Reproduction*, *59*(3), 670–675. https://doi.org/10.1095/biolreprod59.3.670

Charlesworth, D. (2016). The status of supergenes in the 21st century: Recombination suppression in Batesian mimicry and sex chromosomes and other complex adaptations. *Evolutionary Applications*, *9*(1), 74–90. https://doi.org/10.1111/eva.12291

Chen, M., Duan, C., Yin, X., Li, X., Liu, X., Zhang, L., Yue, S., Zhang, Y., & Liu, Y. (2023). Prolactin inhibitor changes testosterone production, testicular morphology, and related genes expression in cashmere goats. *Frontiers in Veterinary Science*, *10*, 1249189. https://doi.org/10.3389/fvets.2023.1249189

Chen, X., Weaver, J., Bove, B. A., Vanderveer, L. A., Weil, S. C., Miron, A., Daly, M. B., & Godwin, A. K. (2008). Allelic imbalance in BRCA1 and BRCA2 gene expression is associated with an increased breast cancer risk. *Human Molecular Genetics*, *17*(9), 1336–1348. https://doi.org/10.1093/hmg/ddn022

Christensen, D., & Vleck, C. M. (2008). Prolactin release and response to vasoactive intestinal peptide in an opportunistic breeder, the zebra finch (Taeniopygia guttata). *General and Comparative Endocrinology*, *157*(2), 91–98.

Cunha, A. A. P., Partridge, C. G., Knapp, R., & Neff, B. D. (2019). Androgen and prolactin manipulation induces changes in aggressive and nurturing behavior in a fish with male parental care. *Hormones and Behavior*, *116*, 104582. https://doi.org/10.1016/j.yhbeh.2019.104582

Davis, J. K., Mittel, L. B., Lowman, J. J., Thomas, P. J., Maney, D. L., Martin, C. L., NISC Comparative Sequencing Program, & Thomas, J. W. (2011). Haplotype-based genomic sequencing of a chromosomal polymorphism in the white-throated sparrow (*Zonotrichia albicollis*). *Journal of Heredity*, *102*(4), 380–390.

Eden, S., & Cedar, H. (1994). Role of DNA methylation in the regulation of transcription. *Current Opinion in Genetics & Development*, *4*(2), 255–259. https://doi.org/10.1016/S0959-437X(05)80052-8

El Halawani, M. E., Silsby, J. L., & Mauro, L. J. (1990). Vasoactive intestinal peptide is a hypothalamic prolactin-releasing neuropeptide in the turkey (*Meleagris gallopavo*). *General and Comparative Endocrinol*, *78*(1), 66–73. https://doi.org/10.1016/0016-6480(90)90048-q

El Halawani, M. E., Whiting, S. E., Silsby, J. L., Pitts, G. R., & Chaiseha, Y. (2000). Active immunization with vasoactive intestinal peptide in turkey hens. *Poultry Science*, *79*(3), 349–354. https://doi.org/10.1093/ps/79.3.349

Falls, J. B., & Kopachena, J. G. (2020). White-throated Sparrow (Zonotrichia albicollis), version 1.0. In A. F. Poole (Ed.), *Birds of the World*. Cornell Lab of Ornithology, Ithaca, NY, USA. https://doi.org/10.2173/bow.whtspa.01

Farrar, V. S., Harris, R. M., Austin, S. H., Nava Ultreras, B. M., Booth, A. M., Angelier, F., Lang, A. S., Feustel, T., Lee, C., Bond, A., MacManes, M. D., & Calisi, R. M. (2022). Prolactin and prolactin receptor expression in the HPG axis and crop during parental care in both sexes of a biparental bird (Columba livia). *General and Comparative Endocrinology*, *315*, 113940. https://doi.org/10.1016/j.ygcen.2021.113940

Friard, O., & Gamba, M. (2016). BORIS: A free, versatile open-source event-logging software for video/audio coding and live observations. *Methods in Ecology and Evolution*, *7*(11), 1325–1330. https://doi.org/10.1111/2041-210X.12584

Gamer, M., & Lemon, J. (2019). *irr: Various Coefficients of Interrater Reliability and Agreement* (v0.84.1) [R]. https://CRAN.R-project.org/package=irr

Goldsmith, A. R. (1982). Plasma concentrations of prolactin during incubation and parental feeding throughout repeated breeding cycles in canaries (*Serinus canarius*). *Journal of Endocrinology*, *94*(1), 51. https://doi.org/10.1677/joe.0.0940051

Goodson, J. L. (2005). The vertebrate social behavior network: Evolutionary themes and variations. *Hormones and Behavior*, *48*(1), 11–22. https://doi.org/10.1016/j.yhbeh.2005.02.003

Goodson, J. L., Kelly, A. M., Kingsbury, M. A., & Thompson, R. R. (2012a). An aggression-specific cell type in the anterior hypothalamus of finches. *Journal of Proceedings of the National Academy of Sciences*, *109*(34), 13847–13852.

Goodson, J. L., Wilson, L. C., & Schrock, S. E. (2012b). To flock or fight: Neurochemical signatures of divergent life histories in sparrows. *Proceedings of the National Academy of Sciences*, *109*(Supplement 1), 10685–10692. https://doi.org/10.1073/pnas.1203394109

Grogan, K. E., Horton, B. M., Hu, Y., & Maney, D. L. (2019). A chromosomal inversion predicts the expression of sex steroid-related genes in a species with alternative behavioral phenotypes. *Molecular and Cellular Endocrinology*, *495*, 110517. https://doi.org/10.1016/j.mce.2019.110517

Hahm, S. H., & Eiden, L. E. (1996). Tissue-specific expression of the vasoactive intestinal peptide gene requires both an upstream tissue specifier element and the 5′ proximal cyclic AMP-responsive element. *Journal of Neurochemistry*, *67*(5), 1872–1881. https://doi.org/10.1046/j.1471-4159.1996.67051872.x

Hahm, S. H., & Eiden, L. E. (1998). Five discrete cis-active domains direct cell type-specific transcription of the vasoactive intestinal peptide (VIP) gene. *Journal of Biological Chemistry*, *273*(27), 17086–17094. https://doi.org/10.1074/jbc.273.27.17086

Hau, M. (2007). Regulation of male traits by testosterone: Implications for the evolution of vertebrate life histories. *BioEssays*, *29*(2), 133–144. https://doi.org/10.1002/bies.20524

Heimovics, S. A., Merritt, J. R., Jalabert, C., Ma, C., Maney, D. L., & Soma, K. K. (2018). Rapid effects of 17β-estradiol on aggressive behavior in songbirds: Environmental and genetic influences. *Hormones and Behavior*, *104*, 41–51. https://doi.org/10.1016/j.yhbeh.2018.03.010

Hellemans, J., Mortier, G., De Paepe, A., Speleman, F., & Vandesompele, J. (2007). qBase relative quantification framework and software for management and automated analysis of real-time quantitative PCR data. *Genome Biology*, *8*(2), R19. https://doi.org/10.1186/gb-2007-8-2-r19

Horton, B. M., Hauber, M. E., & Maney, D. L. (2012). Morph matters: Aggression bias in a polymorphic sparrow. *PLOS ONE*, *7*(10), e48705. https://doi.org/10.1371/journal.pone.0048705

Horton, B. M., & Holberton, R. L. (2010). Morph-specific variation in baseline corticosterone and the adrenocortical response in breeding white-throated sparrows (*Zonotrichia albicollis*). *The Auk*, *127*(3), 540–548. https://doi.org/10.1525/auk.2010.09096

Horton, B. M., Hu, Y., Martin, C. L., Bunke, B. P., Matthews, B. S., Moore, I. T., Thomas, J. W., & Maney, D. L. (2013). Behavioral characterization of a white-throated sparrow homozygous for the ZAL2^{m} chromosomal rearrangement. *Behavior Genetics*, *43*(1), 60–70. https://doi.org/10.1007/s10519-012-9574-6

Horton, B. M., Hudson, W. H., Ortlund, E. A., Shirk, S., Thomas, J. W., Young, E. R., Zinzow-Kramer, W. M., & Maney, D. L. (2014a). Estrogen receptor α polymorphism in a species

with alternative behavioral phenotypes. *Proceedings of the National Academy of Sciences*, *111*(4), 1443–1448.

Horton, B. M., Michael, C. M., Prichard, M. R., & Maney, D. L. (2020a). Vasoactive intestinal peptide as a mediator of the effects of a supergene on social behaviour. *Proceedings of the Royal Society B: Biological Sciences*, *287*(1924), 20200196. https://doi.org/doi:10.1098/rspb.2020.0196

Horton, B. M., Moore, I. T., & Maney, D. L. (2014b). New insights into the hormonal and behavioural correlates of polymorphism in white-throated sparrows, *Zonotrichia albicollis*. *Animal Behavior*, *93*, 207–219.

Horton, B. M., Ryder, T. B., Moore, I. T., & Balakrishnan, C. N. (2020b). Gene expression in the social behavior network of the wire-tailed manakin (*Pipra filicauda*) brain. *Genes, Brain and Behavior*, *19*(1), e12560. https://doi.org/10.1111/gbb.12560

Hunger, L., Kumar, A., & Schmidt, R. (2020). Abundance compensates kinetics: Similar effect of dopamine signals on D1 and D2 receptor populations. *The Journal of Neuroscience*, *40*(14), 2868–2881. https://doi.org/10.1523/JNEUROSCI.1951-19.2019

Huynh, L. Y., Maney, D. L., & Thomas, J. W. (2011). Chromosome-wide linkage disequilibrium caused by an inversion polymorphism in the white-throated sparrow (*Zonotrichia albicollis*). *Journal of Heredity*, *106*(4), 537.

Jongsomjit, D., Jones, S. L., Gerdali, T., Geupel, G. R., & Gouse, P. J. (2007). *A Guide to Nestling Development and Aging in Altricial Passerines*. U.S. Fish and Wildlife Service. https://digitalcommons.unl.edu/cgi/viewcontent.cgi?article=1160&context=usfwspubs

Ketterson, E. D., & Nolan, V. (1994). Male parental behavior in birds. *Annual Review of Ecology and Systematics*, *25*(1), 601–628.

Kindler, P. M., Bahr, J. M., Gross, M. R., & Philipp, D. P. (1991). Hormonal regulation of parental care behavior in nesting male bluegills: Do the effects of bromocriptine suggest a role for prolactin? *Physiological Zoology*, *64*(1), 310–322. https://doi.org/10.1086/physzool.64.1.30158526

Kingsbury, M. A. (2015). New perspectives on vasoactive intestinal polypeptide as a widespread modulator of social behavior. *Currrent Opinion in Behavioral Sciences*, *6*, 139–147. https://doi.org/10.1016/j.cobeha.2015.11.003

Kingsbury, M. A., Jan, N., Klatt, J. D., & Goodson, J. L. (2015). Nesting behavior is associated with VIP expression and VIP–Fos colocalization in a network-wide manner. *Hormones and Behavior*, *69*, 68–81. https://doi.org/10.1016/j.yhbeh.2014.12.010

Kingsbury, M. A., & Wilson, L. C. (2016). The role of VIP in social behavior: Neural hotspots for the modulation of affiliation, aggression, and parental care. *Journal of Integrative and Comparative Biology*, *56*(6), 1238–1249.

Klimaschewski, L. (1997). VIP – a 'Very Important Peptide' in the sympathetic nervous system? *Anatomy and Embryology*, *196*(4), 269–277. https://doi.org/10.1007/s004290050096

Knapton, R. W., & Falls, J. B. (1983). Differences in parental contribution among pair types in the polymorphic white-throated sparrow. *Canadian Journal of Zoology*, *61*(6), 1288–1292. https://doi.org/10.1139/z83-173

Komsta, L. (2022). *outliers: Tests for Outliers* (v0.15) [R]. https://CRAN.R-project.org/package=outliers

Koo, T. K., & Li, M. Y. (2016). A guideline of selecting and reporting intraclass correlation coefficients for reliability research. *Journal of Chiropractic Medicine*, *15*(2), 155–163. https://doi.org/10.1016/j.jcm.2016.02.012

Kopachena, J. G., & Falls, J. B. (1993a). Aggressive performance as a behavioral correlate of plumage polymorphism in the white-throated sparrow (*Zonotrichia albicollis*). *Behaviour*, *124*(3/4), 249–266.

Kopachena, J. G., & Falls, J. B. (1993b). Re-evaluation of morph-specific variations in parental behavior of the white-throated sparrow. *The Wilson Bulletin*, 48–59.

Kosonsiriluk, S., Sartsoongnoen, N., Chaiyachet, O., Prakobsaeng, N., Songserm, T., Rozenboim, I., Halawani, M. E., & Chaiseha, Y. (2008). Vasoactive intestinal peptide and its role in continuous and seasonal reproduction in birds. *General and Comparative Endocrinology*, *159*(1), 88–97. https://doi.org/10.1016/j.ygcen.2008.07.024

Kuenzel, W. J., & Blähser, S. (1994). Vasoactive intestinal polypeptide (VIP)-containing neurons: Distribution throughout the brain of the chick (*Gallus domesticus*) with focus upon the lateral septal organ. *Cell and Tissue Research*, *275*(1), 91–107. https://doi.org/10.1007/BF00305378

Kuenzel, W. J., McCune, S. K., Talbot, R. T., Sharp, P. J., & Hill, J. M. (1997). Sites of gene expression for vasoactive intestinal polypeptide throughout the brain of the chick (*Gallus domesticus*). *Journal of Comparative Neurology*, *381*(1), 101–118. https://doi.org/10.1002/(sici)1096-9861(19970428)381:1<101::Aid-cne8>3.0.Co;2-5

Kulick, R. S., Chaiseha, Y., Kang, S. W., Rozenboim, I., & El Halawani, M. E. (2005). The relative importance of vasoactive intestinal peptide and peptide histidine isoleucine as physiological regulators of prolactin in the domestic turkey. *General and Comparative Endocrinology*, *142*(3), 267–273.

Lasaga, M., Duvilanski, B. H., Seilicovich, A., Afione, S., Diaz, M. del C., Pisera, D., Traktenberg, R., & Debeljuk, L. (1991). The effect of gonadal steroids on vasoactive

intestinal peptide concentration and release from mediobasal hypothalamus and the anterior pituitary gland. *Journal of Neuroendocrinology*, *3*(1), 75–78. https://doi.org/10.1111/j.1365-2826.1991.tb00242.x

Lenth, R. (2023). *emmeans: Estimated Marginal Means, aka Lease-Squares Means* (v1.8.7) [R]. https://CRAN.R-project.org/package=emmeans

Lipshutz, S. E., George, E. M., Bentz, A. B., & Rosvall, K. A. (2019). Evaluating testosterone as a phenotypic integrator: From tissues to individuals to species. *Molecular and Cellular Endocrinology*, *496*, 110531. https://doi.org/10.1016/j.mce.2019.110531

Lowther, J. K. (1961). Polymorphism in the white-throated sparrow, *Zonotrichia albicollis* (GMELIN). *Canadian Journal of Zoology*, *39*(3), 281–292. https://doi.org/10.1139/z61-031

Lynn, S. E. (2016). Endocrine and neuroendocrine regulation of fathering behavior in birds. *Hormones and Behavior*, *77*, 237–248. https://doi.org/10.1016/j.yhbeh.2015.04.005

Macnamee, M. C., Sharp, P. J., Lea, R. W., Sterling, R. J., & Harvey, S. (1986). Evidence that vasoactive intestinal polypeptide is a physiological prolactin-releasing factor in the bantam hen. *General and Comparative Endocrinology*, *62*(3), 470–478. https://doi.org/10.1016/0016-6480(86)90057-2

Mamrut, S., Harony, H., Sood, R., Shahar-Gold, H., Gainer, H., Shi, Y. J., Barki-Harrington, L., & Wagner, S. (2013). DNA methylation of specific CpG sites in the promoter region regulates the transcription of the mouse oxytocin receptor. *PLOS ONE*, *8*(2), e56869. https://doi.org/10.1371/journal.pone.0056869

Maney, D. L. (2008). Endocrine and genomic architecture of life history trade-offs in an avian model of social behavior. *General and Comparative Endocrinology*, *157*(3), 275–282. https://doi.org/10.1016/j.ygcen.2008.03.023

Maney, D. L., & Küpper, C. (2022). Supergenes on steroids. *Philosophical Transactions of the Royal Society B: Biological Sciences*, *377*(1855), 20200507. https://doi.org/10.1098/rstb.2020.0507

Maney, D. L., Lange, H. S., Raees, M. Q., Reid, A. E., & Sanford, S. E. (2009). Behavioral phenotypes persist after gonadal steroid manipulation in white-throated sparrows. *Hormones and Behavior*, *55*(1), 113–120. https://doi.org/10.1016/j.yhbeh.2008.09.002

Maney, D. L., Merritt, J. R., Prichard, M. R., Horton, B. M., & Yi, S. V. (2020). Inside the supergene of the bird with four sexes. *Hormones and Behavior*, *126*, 104850. https://doi.org/10.1016/j.yhbeh.2020.104850

Maney, D. L., Schoech, S. J., Sharp, P. J., & Wingfield, J. C. (1999). Effects of vasoactive intestinal peptide on plasma prolactin in passerines. *Journal of General and Comparative Endocrinology*, *113*(3), 323–330.

Massaro, M., Setiawan, A. N., & Davis, L. S. (2007). Effects of artificial eggs on prolactin secretion, steroid levels, brood patch development, incubation onset and clutch size in the yellow-eyed penguin (*Megadyptes antipodes*). *General and Comparative Endocrinology*, *151*(2), 220–229. https://doi.org/10.1016/j.ygcen.2007.01.034

Mather, K. (1955). Polymorphism as an outcome of disruptive selection. *Evolution*, *9*(1), 52–61. https://doi.org/10.1111/j.1558-5646.1955.tb01513.x

Mello, C. V., Kaser, T., Buckner, A. A., Wirthlin, M., & Lovell, P. V. (2019). Molecular architecture of the zebra finch arcopallium. *Journal of Comparative Neurology*, *527*(15), 2512–2556. https://doi.org/10.1002/cne.24688

Merritt, J. R., Davis, M. T., Jalabert, C., Libecap, T. J., Williams, D. R., Soma, K. K., & Maney, D. L. (2018). Rapid effects of estradiol on aggression depend on genotype in a species with an estrogen receptor polymorphism. *Hormones and Behavior*, *98*, 210–218. https://doi.org/10.1016/j.yhbeh.2017.11.014

Merritt, J. R., Grogan, K. E., Zinzow-Kramer, W. M., Sun, D., Ortlund, E. A., Yi, S. V., & Maney, D. L. (2020). A supergene-linked estrogen receptor drives alternative phenotypes in a polymorphic songbird. *Proceedings of the National Academy of Sciences*, 202011347. https://doi.org/10.1073/pnas.2011347117

Montagne, M., Dussaillant, M., Chew, L., Berod, A., Lamberts, S. J., Cartert, D. A., & Rostene, W. (1995). Estradiol induces vasoactive intestinal peptide and prolactin gene expression in the rat anterior pituitary independently of plasma prolactin levels. *Journal of Neuroendocrinology*, *7*(3), 225–231. https://doi.org/10.1111/j.1365-2826.1995.tb00751.x

Montagnese, C. M., Székely, T., Csillag, A., & Zachar, G. (2015). Distribution of vasotocin- and vasoactive intestinal peptide-like immunoreactivity in the brain of blue tit (*Cyanistes coeruleus*). *Frontiers in Neuroanatomy*, *9*, 90–90. https://doi.org/10.3389/fnana.2015.00090

Niepoth, N., & Bendesky, A. (2020). How natural genetic variation shapes behavior. *Annual Review of Genomics and Human Genetics*, *21*(1), 437–463. https://doi.org/10.1146/annurev-genom-111219-080427

Nishikawa, H., Iijima, T., Kajitani, R., Yamaguchi, J., Ando, T., Suzuki, Y., Sugano, S., Fujiyama, A., Kosugi, S., Hirakawa, H., Tabata, S., Ozaki, K., Morimoto, H., Ihara, K., Obara, M., Hori, H., Itoh, T., & Fujiwara, H. (2015). A genetic mechanism for female-limited Batesian mimicry in Papilio butterfly. *Nature Genetics*, *47*(4), 405–409. https://doi.org/10.1038/ng.3241

Okhovat, M., Berrio, A., Wallace, G., Ophir, A. G., & Phelps, S. M. (2015). Sexual fidelity trade-offs promote regulatory variation in the prairie vole brain. *Science*, *350*(6266), 1371–1374. https://doi.org/10.1126/science.aac5791

Okhovat, M., Maguire, S. M., & Phelps, S. M. (2017). Methylation of avpr1a in the cortex of wild prairie voles: Effects of CpG position and polymorphism. *Royal Society Open Science*, *4*(1), 160646. https://doi.org/10.1098/rsos.160646

Palkovits, M. (1985). Microdissection of individual brain nuclei and areas. In A. A. Boulton & G. B. Baker (Eds.), *General Neurochemical Techniques* (pp. 1–17). Humana Press.

Pinheiro, J. C., & Bates, D. M. (2000). *Mixed-Effects Models in S and S-PLUS*. Springer-Verlag. https://doi.org/10.1007/b98882

Pinheiro, J. C., & Bates, D. M. (2023). *nlme: Linear and Nonlinear Mixed Effects Models* (v3.1-162) [R]. https://CRAN.R-project.org/package=nlme

Prichard, M. R., Grogan, M. E., Merritt, J. R., Root, J., & Maney, D. L. (2022). Allele-specific cis-regulatory methylation of the gene for vasoactive intestinal peptide in white-throated sparrows. *Genes, Brain and Behavior*, *21*(8), e12831. https://doi.org/10.1111/gbb.12831

Purcell, J., Lagunas-Robles, G., Rabeling, C., Borowiec, M. L., & Brelsford, A. (2021). The maintenance of polymorphism in an ancient social supergene. *Molecular Ecology*, *n/a*(n/a). https://doi.org/10.1111/mec.16196

R Core Team. (2023). *R: A Language and Environment for Statistical Computing* [Computer software]. R Foundation for Statistical Computing. https://www.R-project.org

Richfield, E. K. (1989). Anatomical and affinity state comparisons between dopamine D1 and D2, receptors in the rat central nervous system. *Neuroscience*, *30*(3), 767–777.

Roberts, R. L., Jenkins, K. T., Lawler, T., Wegner, F. H., & Newman, J. D. (2001). Bromocriptine administration lowers serum prolactin and disrupts parental responsiveness in common marmosets (*Callithrix j. jacchus*). *Hormones and Behavior*, *39*(2), 106–112. https://doi.org/10.1006/hbeh.2000.1639

Rosvall, K. A., Bergeon Burns, C. M., Barske, J., Goodson, J. L., Schlinger, B. A., Sengelaub, D. R., & Ketterson, E. D. (2012). Neural sensitivity to sex steroids predicts individual differences in aggression: Implications for behavioural evolution. *Proceedings of the Royal Society B: Biological Sciences*, *279*(1742), 3547–3555. https://doi.org/10.1098/rspb.2012.0442

Ruiz-Raya, F., Ibáñez-Álamo, J. D., Parenteau, C., Chastel, O., & Soler, M. (2021). Prolactin mediates behavioural rejection responses to avian brood parasitism. *Journal of Experimental Biology*, *224*(20), jeb240101. https://doi.org/10.1242/jeb.240101

Schwander, T., Libbrecht, R., & Keller, L. (2014). Supergenes and complex phenotypes. *Current Biology*, *24*(7), R288-94. https://doi.org/10.1016/j.cub.2014.01.056

Seiler, H. W., Gahr, M., Goldsmith, A. R., & Guttinger, H. R. (1992). Prolactin and gonadal steroids during the reproductive cycle of the Bengalese finch (*Lonchura striata* var. domestica, Estrildidae), a nonseasonal breeder with biparental care. *General and Comparative Endocrinology*, *88*(1), 83–90. https://doi.org/10.1016/0016-6480(92)90196-q

Sharp, P. J., Dawson, A., & Lea, R. W. (1998). Control of luteinizing hormone and prolactin secretion in birds. *Comparative Biochemistry and Physiology Part C: Pharmacology, Toxicology and Endocrinology*, *119*(3), 275–282. https://doi.org/10.1016/S0742-8413(98)00016-4

Sinervo, B., & Svensson, E. (2002). Correlational selection and the evolution of genomic architecture. *Heredity*, *89*(5), 329–338. https://doi.org/10.1038/sj.hdy.6800148

Sinha, S., Jones, B. M., Traniello, I. M., Bukhari, S. A., Halfon, M. S., Hofmann, H. A., Huang, S., Katz, P. S., Keagy, J., Lynch, V. J., Sokolowski, M. B., Stubbs, L. J., Tabe-Bordbar, S., Wolfner, M. F., & Robinson, G. E. (2020). Behavior-related gene regulatory networks: A new level of organization in the brain. *Proceedings of the National Academy of Sciences*. https://doi.org/10.1073/pnas.1921625117

Smiley, K. O. (2019). Prolactin and avian parental care: New insights and unanswered questions. *Hormones and Behavior*, *11*, 114–130. https://doi.org/10.1016/j.yhbeh.2019.02.012

Smiley, K. O., & Adkins-Regan, E. (2016). Relationship between prolactin, reproductive experience, and parental care in a biparental songbird, the zebra finch (*Taeniopygia guttata*). *General and Comparative Endocrinology*, *232*, 17–24. https://doi.org/10.1016/j.ygcen.2015.11.012

Smiley, K. O., & Adkins-Regan, E. (2018). Lowering prolactin reduces post-hatch parental care in male and female zebra finches (*Taeniopygia guttata*). *Hormones and Behavior*, *98*, 103–114. https://doi.org/10.1016/j.yhbeh.2017.12.011

Spinney, L. H., Bentley, G. E., & Hau, M. (2006). Endocrine correlates of alternative phenotypes in the white-throated sparrow (*Zonotrichia albicollis*). *Hormones and Behavior*, *50*(5), 762–771. https://doi.org/10.1016/j.yhbeh.2006.06.034

Sun, D., Huh, I., Zinzow-Kramer, W. M., Maney, D. L., & Yi, S. V. (2018). Rapid regulatory evolution of a nonrecombining autosome linked to divergent behavioral phenotypes. *Proceedings of the National Academy of Sciences*, *115*(11), 2794–2799. https://doi.org/10.1073/pnas.1717721115

Swett, M. B., & Breuner, C. W. (2008). Interaction of testosterone, corticosterone and corticosterone binding globulin in the white-throated sparrow (*Zonotrichia albicollis*). *Comparative Biochemistry and Physiology Part A: Molecular & Integrative Physiology*, *151*(2), 226–231. https://doi.org/10.1016/j.cbpa.2008.06.031

Talbot, R. T., Hanks, M. C., Sterling, R. J., Sang, H. M., & Sharp, P. J. (1991). Pituitary prolactin messenger ribonucleic acid levels in incubating and laying hens: Effects of manipulating plasma levels of vasoactive intestinal polypeptide. *Endocrinology*, *129*(1), 496–502.

Thierry, A.-M., Brajon, S., Massemin, S., Handrich, Y., Chastel, O., & Raclot, T. (2013). Decreased prolactin levels reduce parental commitment, egg temperatures, and breeding success of incubating male Adélie penguins. *Hormones and Behavior*, *64*(4), 737–747. https://doi.org/10.1016/j.yhbeh.2013.06.003

Thomas, J. W., Caceres, M., Lowman, J. J., Morehouse, C. B., Short, M. E., Baldwin, E. L., Maney, D. L., & Martin, C. L. (2008). The chromosomal polymorphism linked to variation in social behavior in the white-throated sparrow (*Zonotrichia albicollis*) is a complex rearrangement and suppressor of recombination. *Genetics*, *179*(3), 1455–1468. https://doi.org/10.1534/genetics.108.088229

Thompson, M. J., & Jiggins, C. D. (2014). Supergenes and their role in evolution. *Heredity*, *113*(1), 1–8. https://doi.org/10.1038/hdy.2014.20

Thorneycroft, H. B. (1975). A cytogenetic study of the white-throated sparrow, *Zonotrichia albicollis* (Gmelin). *Journal of Evolution*, *29*(4), 611–621.

Trantham-Davidson, H., Neely, L. C., Lavin, A., & Seamans, J. K. (2004). Mechanisms underlying differential D1 versus D2 dopamine receptor regulation of inhibition in prefrontal cortex. *The Journal of Neuroscience*, *24*(47), 10652–10659. https://doi.org/10.1523/JNEUROSCI.3179-04.2004

Trivers, R. (1972). Parental investment and sexual selection. In B. Campbell (Ed.), *Sexual Selection and the Descent of Man* (pp. 139–179). Aldine.

Tuttle, E. M. (2003). Alternative reproductive strategies in the white-throated sparrow: Behavioral and genetic evidence. *Behavioral Ecology*, *14*(3), 425–432.

Tuttle, E. M., Bergland, A. O., Korody, M. L., Brewer, M. S., Newhouse, D. J., Minx, P., Stager, M., Betuel, A., Cheviron, Z. A., Warren, W. C., Gonser, R. A., & Balakrishnan, C. N. (2016). Divergence and functional degradation of a sex chromosome-like supergene. *Current Biology*, *26*(3), 344–350. https://doi.org/10.1016/j.cub.2015.11.069

Valdez, D. J. (2022). An updated look at the mating system, parental care and androgen seasonal variations in ratites. *General and Comparative Endocrinology*, *323–324*, 114034. https://doi.org/10.1016/j.ygcen.2022.114034

Van Roo, B. (2003). Testosterone and prolactin in two songbirds that differ in paternal care: The blue-headed vireo and the red-eyed vireo. *Hormones and Behavior*, *44*(5), 435–441. https://doi.org/10.1016/j.yhbeh.2003.07.001

Wacker, D. W., Schlinger, B. A., & Wingfield, J. C. (2008). Combined effects of DHEA and fadrozole on aggression and neural VIP immunoreactivity in the non-breeding male song

sparrow. *Hormones and Behavior*, *53*(1), 287–294. https://doi.org/10.1016/j.yhbeh.2007.10.008

Watt, D. J., Ralph, C. J., & Atkinson, C. T. (1984). The role of plumage polymorphism in dominance relationships of the white-throated sparrow. *The Auk*, *101*(1), 110–120. https://doi.org/10.1093/auk/101.1.110

Wickham, H. (2009). *ggplot2: Elegant Graphics for Data Analysis*. Springer. https://doi.org/10.1007/978-0-387-98141-3

Wingfield, J. C., & Goldsmith, A. R. (1990). Plasma levels of prolactin and gonadal steroids in relation to multiple-brooding and renesting in free-living populations of the song sparrow, *Melospiza melodia*. *Hormones and Behavior*, *24*(1), 89–103. https://doi.org/10.1016/0018-506X(90)90029-W

Wingfield, J. C., Hegner, R. E., Dufty, A. M., & Ball, G. F. (1990). The "Challenge Hypothesis": Theoretical implications for patterns of testosterone secretion, mating systems, and breeding strategies. *The American Naturalist*, *136*(6), 829–846. https://doi.org/10.1086/285134

Wittkopp, P. J., & Kalay, G. (2011). *Cis*-regulatory elements: Molecular mechanisms and evolutionary processes underlying divergence. *Nature Reviews Genetics*, *13*(1), 59–69. https://doi.org/10.1038/nrg3095

Wray, G. A. (2007). The evolutionary significance of *cis*-regulatory mutations. *Nature Reviews Genetics*, *8*(3), Article 3. https://doi.org/10.1038/nrg2063

Xu, M., Proudman, J. A., Pitts, G. R., Wong, E. A., Foster, D. N., & Halawani, M. E. E. (1996). Vasoactive intestinal peptide stimulates prolactin mRNA expression in turkey pituitary

cells: Effects of dopaminergic drugs. *Experimental Biology and Medicine*, *212*(1), 52–62. https://doi.org/10.3181/00379727-212-43991

Youngren, O. M., Chaiseha, Y., & El Halawani, M. E. (1998). Regulation of prolactin secretion by dopamine and vasoactive intestinal peptide at the level of the pituitary in the turkey. *Neuroendocrinology*, *68*(5), 319–325. https://doi.org/10.1159/000054380

Youngren, O. M., Pitts, G. R., Phillips, R. E., & El Halawani, M. E. (1996). Dopaminergic control of prolactin secretion in the turkey. *General and Comparative Endocrinology*, *104*(2), 225–230. https://doi.org/10.1006/gcen.1996.0165

Zinzow-Kramer, W. M., Horton, B. M., & Maney, D. L. (2014). Evaluation of reference genes for quantitative real-time PCR in the brain, pituitary, and gonads of songbirds. *Hormones and Behavior*, *66*(2), 267–275. https://doi.org/10.1016/j.yhbeh.2014.04.011

Zinzow-Kramer, W. M., Horton, B. M., McKee, C. D., Michaud, J. M., Tharp, G. K., Thomas, J. W., Tuttle, E. M., Yi, S., & Maney, D. L. (2015). Genes located in a chromosomal inversion are correlated with territorial song in white-throated sparrows. *Genes, Brain, and Behavior*, *14*(8), 641–654.

Figures

Figure 1. The white-striped (WS) and tan-striped (TS) morphs and their chromosomes. TS birds of both sexes have muted coloration and are homozygous for the standard chromosome, ZAL2, whereas WS birds of both sexes have bold, bright coloration and carry at least one copy of $ZAL2^{m}$, which contains a large chromosomal inversion, or supergene. Illustration by M. R. Prichard.

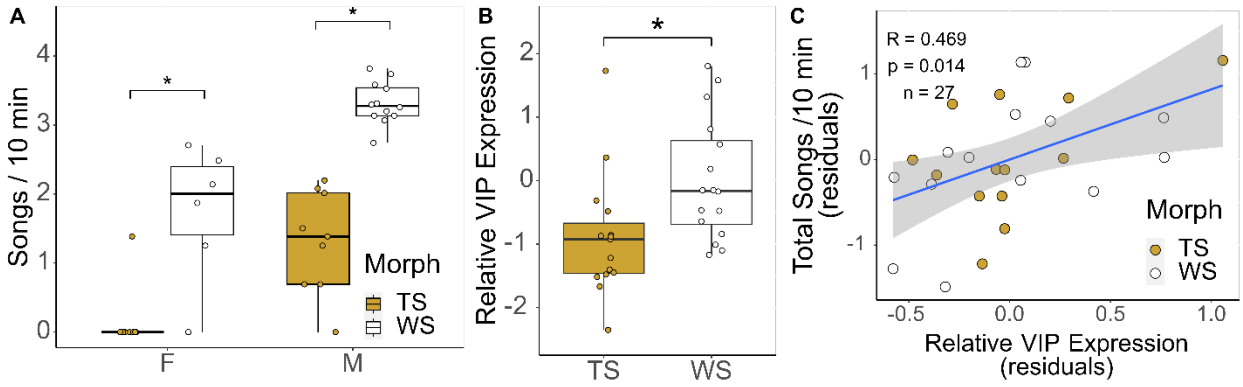

Figure 2. Morph differences in territorial singing and vasoactive intestinal peptide (*VIP*) expression in the anterior hypothalamus (AH), and the correlation between the two, in free-living white-throated sparrows. In all three panels, color corresponds with morph; gold represents tan-striped (TS), and white represents white-striped (WS) birds. The data in these figures are limited to the pre-parental cohort. (A) The x-axis separates males (M) and females (F), and the y-axis indicates the occurrence of aggressive behavior measured as total songs per 10-minute stimulated territorial intrusion (STI). The data in this panel are $\log_{10}$ transformed. (B) The x-axis indicates morph, and the y-axis indicates the amount of *VIP* expression in the AH. The data in this panel are $\log_2$ transformed. (C) The x-axis indicates relative *VIP* expression in the AH, and the y-axis indicates singing in response to an STI. Plotted values are residuals controlling for morph, sex, date, and qPCR run. For the correlation between territorial singing and *VIP* expression in a different brain region, the infundibular nucleus (IN), see Figure S1, and for complete statistical results, see Table S3.

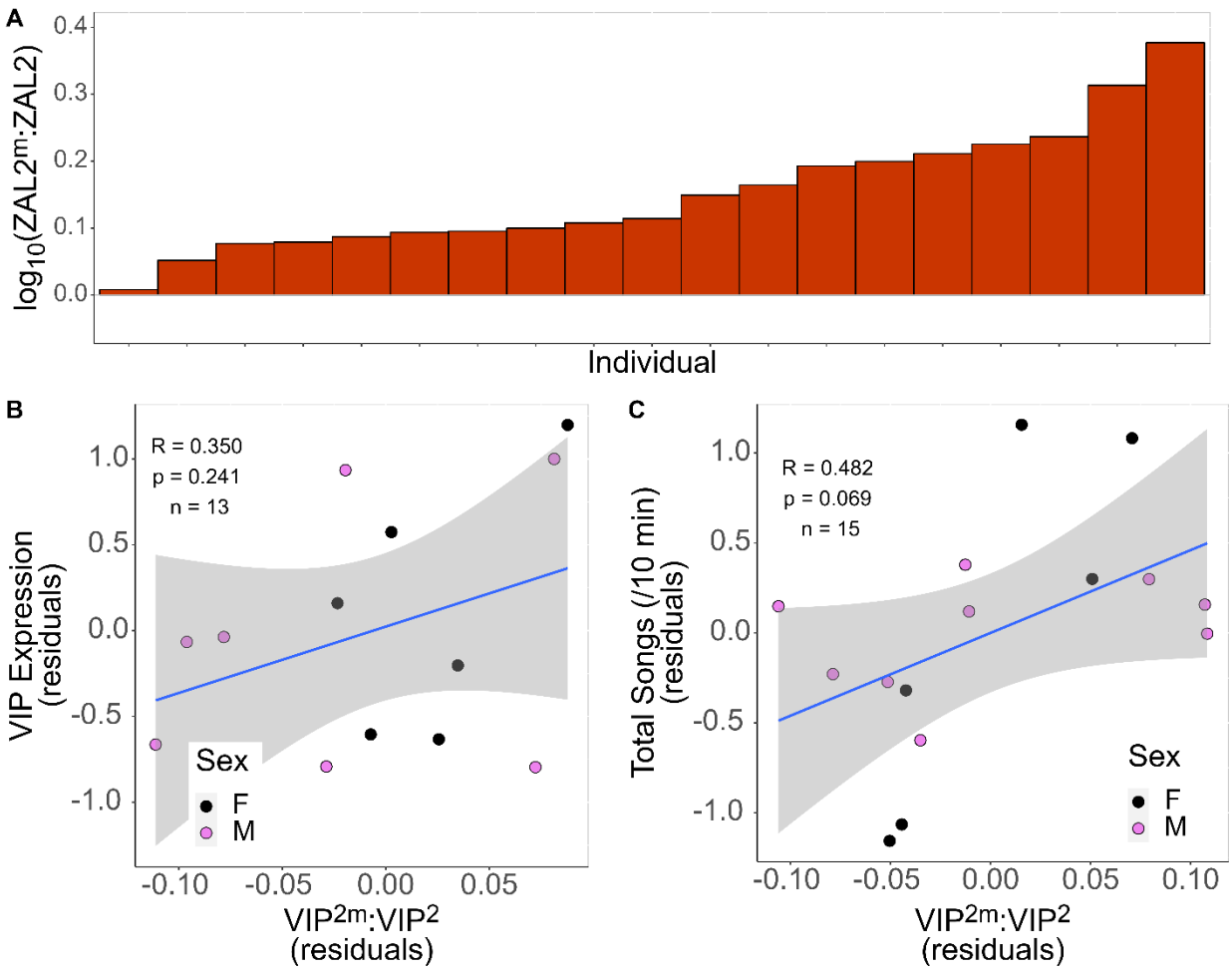

Figure 3. Allelic imbalance in the AH of the pre-parental cohort. (A) The *ZAL2^{m}* allele of vasoactive intestinal peptide (*VIP^{2m}*) is overexpressed relative to the ZAL2 allele of *VIP* (*VIP^{2}*) in the anterior hypothalamus (AH). The y-axis in this figure indicates the degree of allelic imbalance, which is the ratio of the expression of the ZAL2^{m} allele (*VIP^{2m}*) to the ZAL2 allele (*VIP^{2}*) of *VIP*. The data are $\log_{10}$ transformed so that zero represents equal expression of the alleles on the y-axis. Each bar represents the degree of allelic imbalance in the AH of an individual bird; in this case, all birds showed over-expression of VIP^{2m} relative to VIP^{2}. (B) The correlation is shown between the degree of allelic imbalance in the AH (x-axis) and overall *VIP* expression in the AH (y-axis). The color of each point corresponds with sex; violet is male (M)

and black is female (F). All plotted values are residuals controlling for sex, date, and year. (C) The correlation is shown between allelic imbalance in the AH and territorial singing. The color of each point corresponds with sex; violet is male (M) and black is female (F). For the correlation between allelic imbalance in a different brain region, the infundibular nucleus, and territorial singing see Figure S2. All plotted values are residuals controlling for sex, date, and year. See Table S4 for complete statistical results.

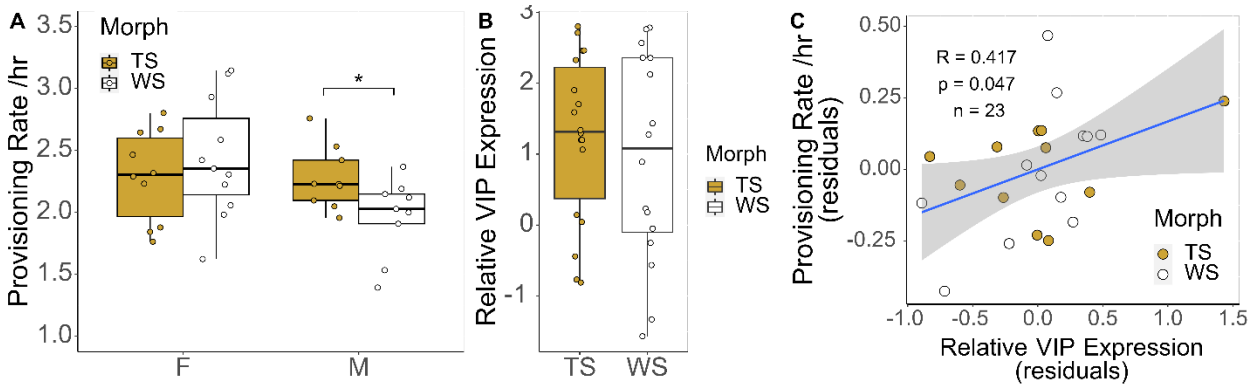

Figure 4. Morph differences in nestling provisioning and vasoactive intestinal peptide (*VIP*) expression in the infundibular nucleus (IN), and the correlation between the two, in free-living white-throated sparrows. In all three panels, color corresponds with morph; gold represents tan-striped (TS), and white represents white-striped (WS) birds. The data in these figures are limited to the parental cohort. (A) The x-axis separates males (M) and females (F), and the y-axis indicates parental behavior measured as provisioning trips per hour of video. The data in this panel are square root transformed. (B) The x-axis separates the TS and WS morphs, and the y-axis indicates the amount of *VIP* expression in the IN. The data in this panel are $\log_2$ transformed. (C) The x-axis indicates the relative amount of *VIP* expression in the IN, and the y-axis indicates provisioning rate. Plotted values are residuals controlling for morph, sex, date, and qPCR run. For the correlation between nestling provisioning and *VIP* expression in a different brain region, the anterior hypothalamus (AH), see Figure S3, and for complete statistical results for these figures, see Table S6.

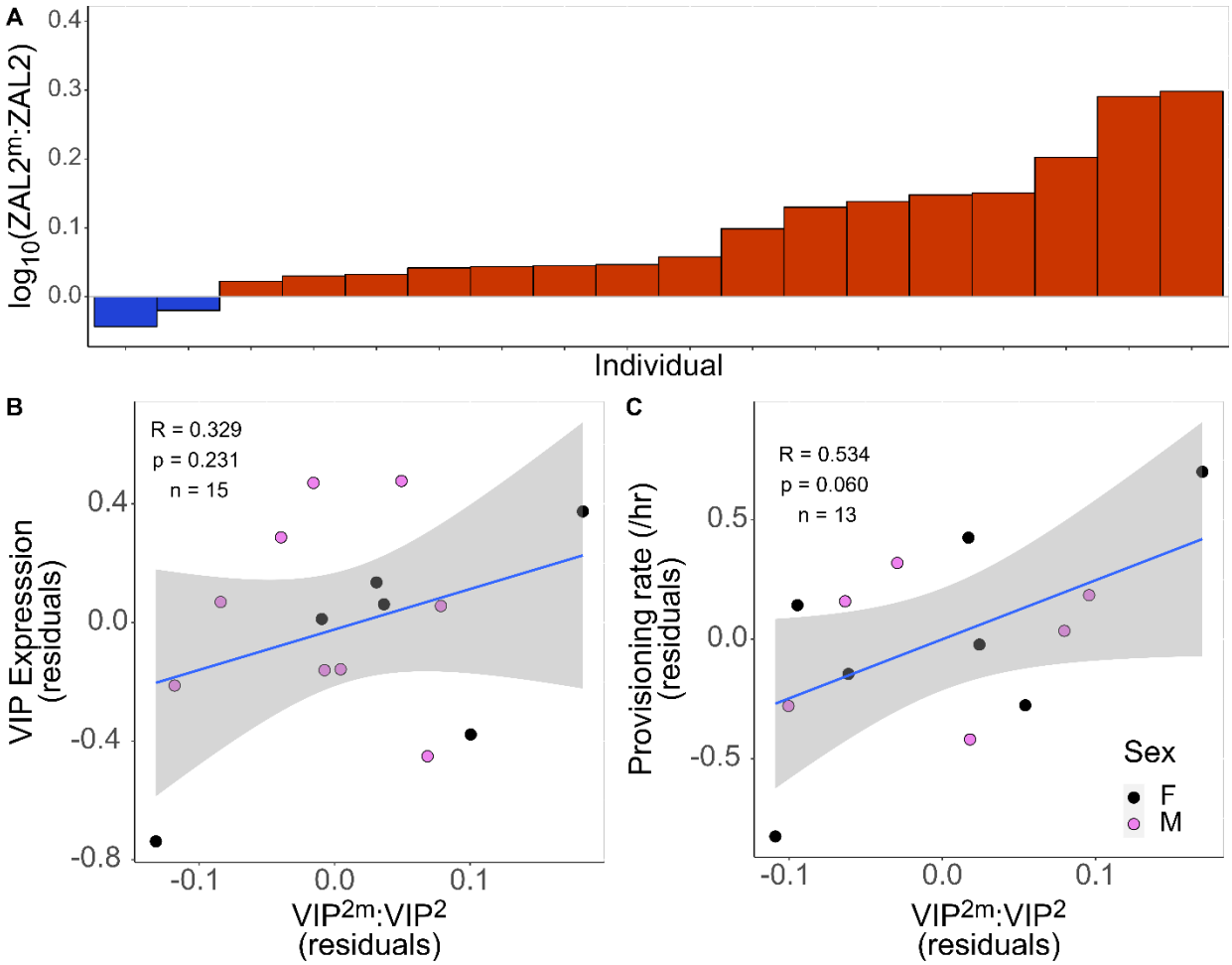

Figure 5. Allelic imbalance in the IN of the parental cohort. (A) The *ZAL2*^{m} allele of vasoactive intestinal peptide (*VIP*^{2m}) is overexpressed relative to the ZAL2 allele of *VIP* (*VIP*^{2}) in the infundibular nucleus (IN). The y-axis in this figure indicates the degree of allelic imbalance, which is the ratio of the expression of the ZAL2^{m} allele (*VIP*^{2m}) to the ZAL2 allele (*VIP*^{2}) of *VIP*. The data are $\log_{10}$ transformed, so that zero represents equal expression of the alleles on the y-axis. Each bar represents the degree of allelic imbalance in the AH of an individual bird, and the color indicates which allele was overexpressed in that individual; above zero is colored red and indicates overexpression of *VIP*^{2m} and below zero in blue indicates over-expression of *VIP*^{2}. (B) The correlation is shown between the degree of allelic imbalance in the IN (x-axis) and

overall *VIP* expression in the IN (y-axis) in the pre-parental cohort only. The color of each point corresponds with sex; violet is male (M) and black is female (F). All plotted values are residuals controlling for sex, date, and year. (C) The positive correlation is shown between allelic imbalance in the IN and nestling provisioning was not significant. The color of each point corresponds with sex; violet is male (M) and black is female (F). For the correlation of allelic imbalance in a different brain region, the anterior hypothalamus, and provisioning rate see Figure S4. All plotted values are residuals controlling for sex, date, and year. See Table S7 for complete statistical results.

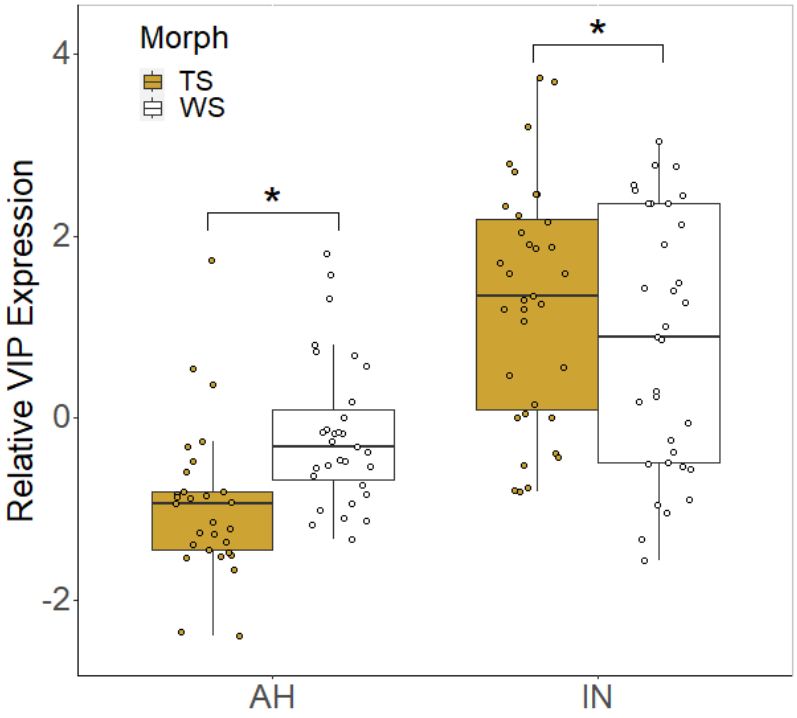

Figure 6. Morph differences in *VIP* expression depended on brain region. The morph difference in vasoactive intestinal peptide (*VIP*) expression in the anterior hypothalamus (AH) went in a direction opposite from the morph difference in the infundibular nucleus (IN) after pooling the pre-parental and parental cohorts of animals. The colors of the boxes in this plot correspond with morph; gold refers to tan-striped (TS) and white to white-striped (WS) birds. The y-axis indicates the level of *VIP* expression, which is $\log_2$ transformed. Asterisks (*) denote $p < 0.05$ in *post-hoc* tests for morph differences within brain region and with sexes pooled. For complete statistical results, see Table S8.

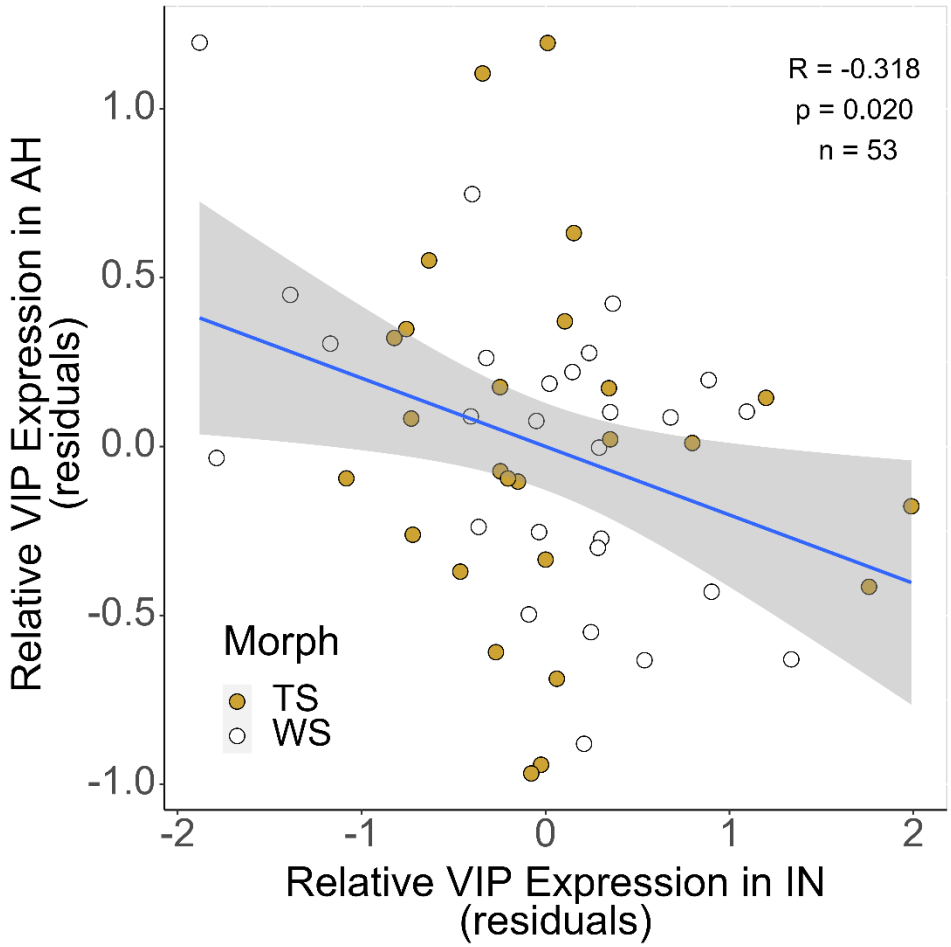

Figure 7. VIP expression in the AH and IN were negatively correlated. There was a negative relationship between vasoactive intestinal peptide (*VIP*) expression in the anterior hypothalamus (AH) and *VIP* expression in the infundibular nucleus (IN) with the pre-parental and parental cohorts pooled. The color of the symbols corresponds with morphs: gold refers to tan-striped (TS) and white to white-striped (WS) birds. Plotted values are residuals after controlling for morph, sex, date, and qPCR run.

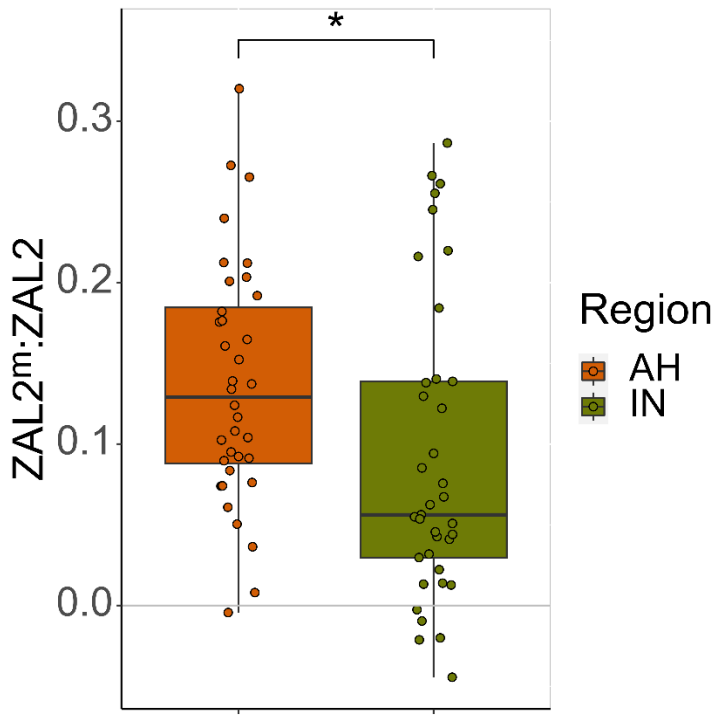

Figure 8. Allelic imbalance in *VIP* expression differs between the AH and IN. Results from the allelic imbalance assay show differential expression of the alleles of vasoactive intestinal peptide (*VIP*) in the anterior hypothalamus (AH) and the infundibular nucleus (IN). The y-axis in both figures indicates the degree of allelic imbalance, which is the ratio of the expression of the ZAL2^{m} allele (VIP^{2m}) to the ZAL2 allele (VIP^{2}) of *VIP*. The data are $\log_{10}$ transformed in the plots so that equal expression of the alleles, or a 1:1 ratio, is at zero on the y-axis; above zero indicates overexpression of VIP^{2m} relative to $VIP^{2,}$ and below zero indicates under-expression of VIP^{2m} relative to VIP^{2}. The orange box is the allelic imbalance in the AH, and the green is the IN. For complete statistical results, see Table S8.

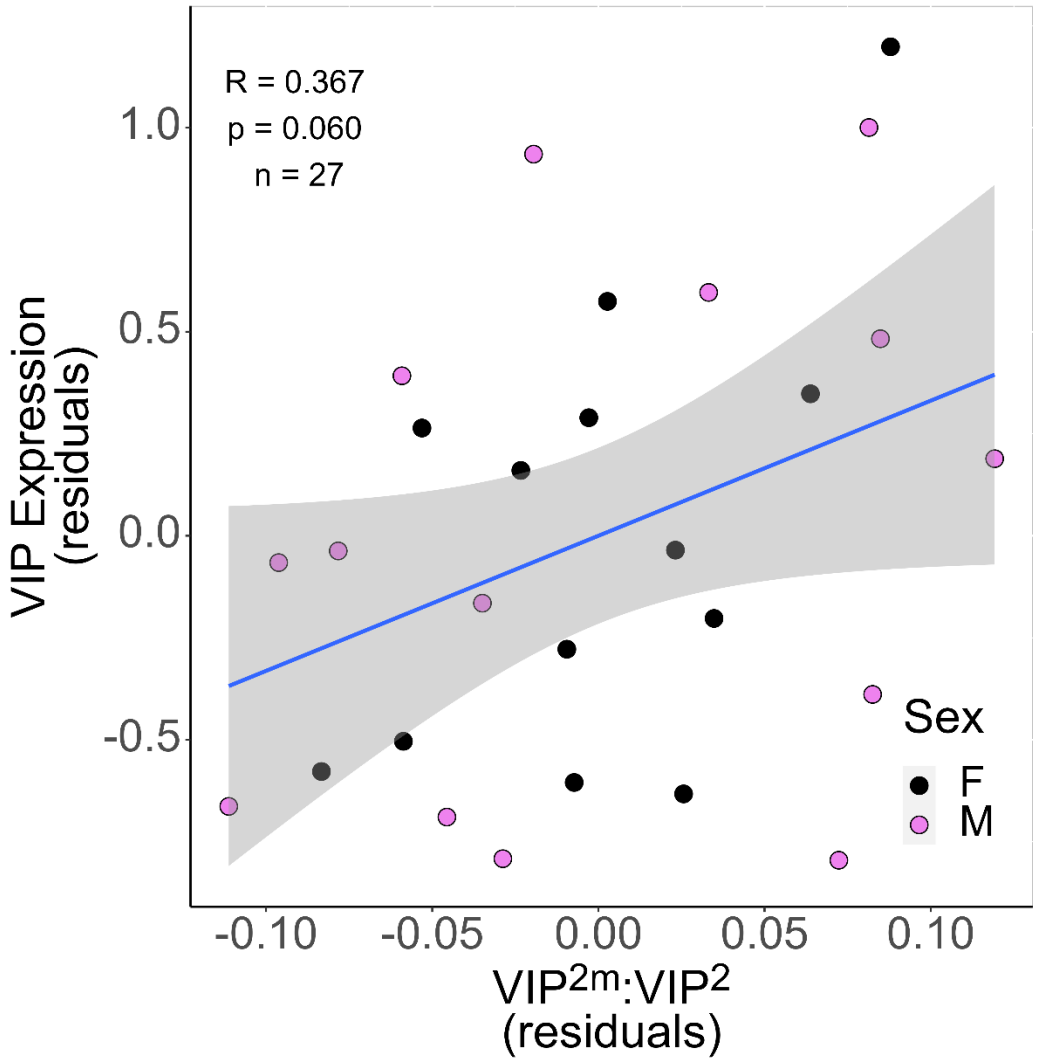

Figure 9. Correlation between allelic imbalance and overall expression of *VIP* in the AH with the cohorts pooled. In the anterior hypothalamus (AH), allelic imbalance positively predicted the amount of vasoactive intestinal peptide (*VIP*) expression with the pre-parental and parental cohorts pooled. The color corresponds with sex; violet is male (M), and black is female (F). All plotted values are residuals controlling for sex, date, and year. See Table S4 for complete statistical results.

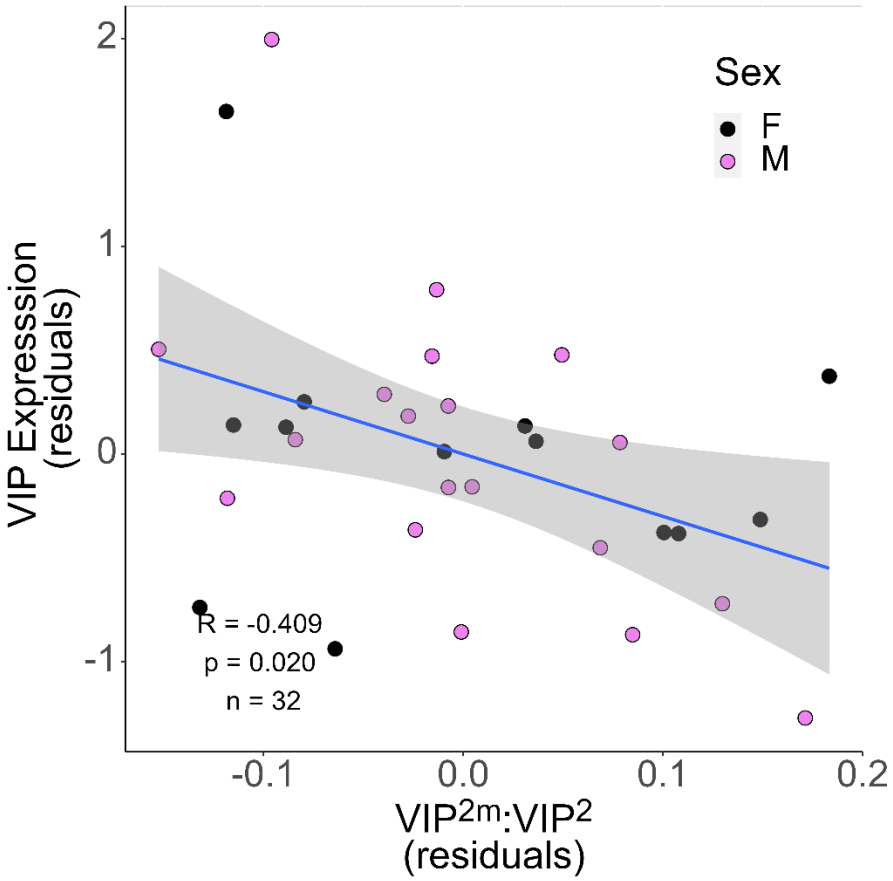

Figure 10. Correlation between allelic imbalance and overall expression of *VIP* in the IN with the cohorts pooled. The degree of allelic imbalance in the infundibular nucleus (IN) correlated negatively with overall vasoactive intestinal peptide (*VIP*) expression in the IN when the pre-parental and parental cohorts were pooled. The color of each point corresponds with sex; violet is male (M), and black is female (F). All plotted values are residuals controlling for sex, date, and year. See Table S7 for complete statistical results.

Appendix

Formulas

E = efficiency; m = slope; g, number of probes/alleles j:j`; s, number of samples, k:k`; Cp = Crossing point / cycle threshold value after taking the arithmetic mean of technical replicates; Cp_{ref} = mean Cp of each gene or primer/probe. RQ = relative quantity; $RQR_{j,j`}$= ratio of the relative quantity of allele/probe j to allele/probe j`; HKG = housekeeping genes; HKG_k = geometric mean of housekeeping genes for a given sample

Efficiency from the slope of the standard curve.

$$Formula\ 1: E_j = 10^{-\frac{1}{m_j}}$$

ΔCp for each sample/gene.

$$Formula\ 2: \Delta Cp = Cp_{ref,j} - Cp_{jk}$$

Linear RQ for each sample and each gene/probe from ΔCp values.

$$Formula\ 3: RQ_{jk} = E_j^{\Delta Cp_j}$$

RQR for each sample.

$$Formula\ 4: RQR_{j:j`} = \frac{RQ_{jk}}{RQ_{j`k}}$$

$$Example\ 1: RQR_{VIP:HKG} = \frac{VIP}{HKG_k} = \frac{RQ_{VIP,k}}{\sqrt{RQ_{GAPDH,k} * RQ_{PPIA,k}}}$$

$$Example\ 2: RQR_{Cy5:FAM} = \frac{Cy5}{FAM} = \frac{RQ_{Cy5,k}}{RQ_{FAM,k}}$$

Supplementary Tables

Sample Sizes (n = 74)

Year	Breeding Stage	Morph	Sex	n
2019 (n = 35)	Pre-parental (n = 20)	WS	M	5
			F	5
		TS	M	5
			F	5
	Parental (n = 15)	WS	M	3
			F	5
		TS	M	4
			F	3
2021 (n = 39)	Pre-parental (n = 18)	WS	M	6
			F	3
		TS	M	6
			F	3
	Parental (n = 21)	WS	M	6
			F	4
		TS	M	5
			F	6

Table S1. Sample sizes within year, breeding stage, morph, and sex. The animals in this study were collected over two summers in 2019 and 2021. During each summer, birds were collected either as part of the pre-parental cohort, which comprised animals evaluated for aggressive behavior before the start of incubation, or as part of the parental cohort, which comprised animals evaluated for parental behavior after the nestlings hatched and before they fledged. The two morphs, white-striped (WS) and tan-striped (TS) (Figure 1), and both sexes, male (M) and female (F), were approximately balanced across the two cohorts within each year.

Latency to Respond to Decoy

Description	Fixed Effect	n	DF	F-value	η^2	p-value
Time from start of playback until the focal animal showed interest in the decoy	Morph	33	27	10.48	0.28	0.003*
	Sex	33	27	1.846	0.06	0.186
	Morph:Sex	33	27	1.244	0.04	0.275

Time w/in 5m

Description	Fixed Effect	n	DF	F-value	η^2	p-value
Duration of time the focal animal spent within a 5m radius of the decoy	Morph	35	29	0.513	0.02	0.479
	Sex	35	29	4.374	0.13	0.045*
	Morph:Sex	35	29	0.001	<0.01	0.973

Time w/in 2m

Description	Fixed Effect	n	DF	F-value	η^2	p-value
Duration of time the focal animal spent within a 2m radius of the decoy	Morph	35	29	0.058	0.02	0.451
	Sex	35	29	1.091	0.04	0.305
	Morph:Sex	35	29	0.529	0.02	0.473

Closest Proximity to Decoy

Description	Fixed Effect	n	DF	F-value	η^2	p-value
The approximate distance in meters of the closest approach to the decoy	Morph	35	29	3.103	0.10	0.089
	Sex	35	29	2.777	0.09	0.106
	Morph:Sex	35	29	0.025	<0.01	0.876

Total Flights

Description	Fixed Effect	n	DF	F-value	η^2	p-value
Total number of flights over, toward, and around the decoy	Morph	35	29	5.440	0.16	0.027*
	Sex	35	29	7.933	0.21	0.009*
	Morph:Sex	35	29	0.544	0.02	0.467

Trills

Description	Fixed Effect	n	DF	F-value	η^2	p-value
A vocalization exhibited during copulation solicitation (typically female) and aggressive encounters (typically male)	Morph	35	29	2.271	0.07	0.143
	Sex	35	29	26.09	0.47	<0.001*
	Morph:Sex	35	29	6.339	0.18	0.018*

Post-hoc tests for morph differences

Sex	n	t-value	p-value
Females	14	-0.833	0.002*
Males	21	-0.019	0.928

Other Vocalizations

Description	Fixed Effect	n	DF	F-value	η^2	p-value
Chips, chip-ups, pinks, etc.	Morph	35	29	0.006	<0.01	0.941
	Sex	35	29	0.001	<0.01	0.975
	Morph:Sex	35	29	1.729	0.06	0.199

Table S2. Morph differences in aggressive/territorial behaviors other than singing. The results in this table are from MANCOVAs and post-hoc analyses of non-song aggressive behaviors (Table

S3) recorded during simulated territorial intrusions (STIs). In *post-hoc* tests for morph differences, a negative t-value indicates tan-striped (TS) > white-striped (WS), and a positive t-value indicates WS > TS. Statistical model: $\log_{10}$(behavior) ~ morph * sex + date + 1|year.

Territorial Singing

Fixed Effect	n	DF	F-value	η^2	p-value
Morph	35	29	97.82	0.77	<0.001*
Sex	35	29	40.57	0.58	<0.001*
Morph:Sex	35	29	1.485	0.05	0.233

Post-hoc morph differences

Sex	n	t-value	p-value
Females	14	-4.659	<0.001*
Males	21	-7.648	<0.001*

***VIP* Expression in AH**

Fixed Effect	n	DF	F-value	η^2	p-value
Morph	31	22	8.289	0.77	0.009*
Sex	31	22	0.035	<0.01	0.855
Morph:Sex	31	22	0.005	<0.01	0.943

***VIP* Expression and Territorial Singing**

Region	n	DF	R	p-value	Fisher's Z
AH	27	25	0.469	0.014*	0.045*
IN	27	25	-0.069	0.733	

Table S3. Morph differences in and correlations between territorial singing and *VIP* expression. This table shows the results from MANCOVA and *post-hoc* analyses that demonstrate the morph difference in aggression and expression of vasoactive intestinal peptide (*VIP*) in the anterior hypothalamus (AH), as well as the results of partial Pearson's correlations, which demonstrate the positive relationship between *VIP* expression in the AH and territorial singing. The data presented above are limited to the pre-parental cohort. Data from the stimulated territorial intrusions (STIs) were $\log_{10}$ transformed, and qPCR data were $\log_2$ transformed to adjust for kurtosis. The statistical models were as follows: territorial behavior: $\log_{10}$(songs) ~ morph * sex + date + 1|year; *VIP* expression: RQR ~ morph * sex + 1|qPCR run; residual model for correlations: ~ morph * sex + date + 1|qPCR run. See Figure 2 and Figure S1 for the corresponding plots of these data.

Allelic Imbalance in *VIP* Expression

Cohort	n	mean	t-value	p-value
Pre-parental	19	0.199	7.628	<0.001*
Parental	17	0.194	7.788	<0.001*

Correlations between Allelic Imbalance and *VIP* Expression

Cohort	n	DF	R	p-value
Both	27	25	0.367	0.060
Pre-parental	13	11	0.350	0.241
Parental	14	12	0.427	0.128

Correlations between Allelic Imbalance and Behavior

Brain Region	n	DF	R	p-value	Fisher's Z
AH	15	13	0.482	0.069	0.200
IN	17	15	0.021	0.937	

Table S4. Allelic imbalance in the AH. In the top part of the table, the results of tests for allelic imbalance, or a ratio different from 1:1, in the expression of vasoactive intestinal peptide (*VIP*) alleles in the anterior hypothalamus (AH) are shown. All tests were one-sample t-tests. The next two parts of the table shows the results of correlations that were conducted on residual values calculated from the following statistical models: allelic imbalance & expression: sex + date + 1|year/qPCR run; allelic imbalance & behavior: sex + date + 1|year. See Figures 3, 9, S2, and S5 for corresponding plots of these data.

Latency to Return to Nest

Description	Fixed Effect	n	DF	F-value	η^2	p-value
Duration (sec) before the focal animal returned to the nest after the disturbance of setting up the camera	Morph	39	32	2.442	0.07	0.128
	Sex	39	32	4.524	0.12	0.041*
	Morph:Sex	39	32	7.930	0.20	0.008*
	Post-hoc morph differences					
	Sex	**n**	**t-value**	**p-value**		
	Females	21	0.797	0.432		
	Males	18	-3.170	0.003*		

Total Visits /hr

Description	Fixed Effect	n	DF	F-value	η^2	p-value
Total number of trips to the nest, either with or without food for the nestlings, per hour of video	Morph	39	32	0.067	<0.01	0.798
	Sex	39	32	5.505	0.15	0.025*
	Morph:Sex	39	32	3.802	0.11	0.060

Proportion of Time Spent at Nest

Description	Fixed Effect	n	DF	F-value	η^2	p-value
Total proportion of time spent at the nest, regardless of activity (e.g., brooding, feeding nestlings, etc)	Morph	39	32	0.025	<0.01	0.875
	Sex	39	32	22.430	0.42	<0.001*
	Morph:Sex	39	32	<0.001	<0.01	0.983

Proportion of Time Spent Brooding

Description	Fixed Effect	n	DF	F-value	η^2	p-value
Total proportion of time spent brooding (i.e., making physical contact with nestlings/brood patch)	Morph	39	32	0.322	<0.01	0.574
	Sex	39	32	16.88	0.35	<0.001*
	Morph:Sex	39	32	0.135	<0.01	0.716

Fecal Sac Removals

Description	Fixed Effect	n	DF	F-value	η^2	p-value
Total count of the number of fecal sacs removed from the nest per hour of video	Morph	39	32	2.915	0.08	0.094
	Sex	39	32	0.129	<0.01	0.722
	Morph:Sex	39	32	4.371	0.12	0.045
	Post-hoc morph differences					
	Sex	**n**	**t-value**	**p-value**		
	Females	21	-0.216	0.830		
	Males	18	2.695	0.011		

Table S5. Morph differences in parental behaviors other than nestling provisioning. The results in this table are from MANCOVAs and *post-hoc* analyses of behaviors other than provisioning rate (Table S5) that were recorded during videos of parental behavior. Data are limited to nestlings that were aged 6-days post-hatch. In *post-hoc* tests for morph differences, a negative t-

value indicates tan-striped (TS) > white-striped (WS), and a positive t-value indicates WS > TS. Statistical model: sqrt(provisioning trips) ~ morph * sex + date + 1|year.

Nestling Provisioning

Fixed Effect	n	DF	F-value	η^2	p-value
Morph	39	32	0.282	<0.01	0.599
Sex	39	32	4.403	0.08	0.044*
Morph:Sex	39	32	5.102	0.16	0.031*

Post-hoc morph differences

Sex	n	t-value	p-value
Females	21	-1.154	0.257
Males	18	2.059	0.048*

***VIP* Expression in IN**

Fixed Effect	n	DF	F-value	η^2	p-value
Morph	34	24	0.079	<0.01	0.791
Sex	34	24	36.01	0.60	<0.001*
Morph:Sex	34	24	0.394	0.02	0.536

Correlations between *VIP* Expression and Nestling Provisioning

Region	n	DF	R	p-value	Fisher's Z
AH	21	19	-0.104	0.655	0.091
IN	23	21	0.417	0.048*	

Table S6. Morph differences in and correlations between nestling provisioning and *VIP* expression. The results in this table are from MANCOVA and *post-hoc* analyses that demonstrate the morph differences in parental care and vasoactive intestinal peptide (*VIP*) expression in the infundibular nucleus (IN). Results of the partial Pearson's correlation demonstrate the positive relationship between *VIP* expression in the IN and nestling provisioning. The data presented above are limited to the parental cohort. Data from the parental videos were square root transformed, and qPCR data were $\log_2$ transformed to adjust for kurtosis. The statistical models were as follows: parental care: sqrt(provisioning trips) ~ morph * sex + date + 1|year; *VIP* expression: $\log_2$(RQR) ~ morph * sex + 1|qPCR run; residual model for correlations: ~ morph * sex + date + 1|qPCR run. See Figure 4 and Figure S3 for the corresponding plots of these data.

Allelic Imbalance in *VIP* Expression

Cohort	n	mean	t-value	p-value
Pre-parental	19	0.138	4.144	<0.001*
Parental	18	0.125	4.304	<0.001*

Correlations between Allelic Imbalance and *VIP* Expression

Cohort	n	DF	R	p-value
Both	33	31	-0.409	0.020*
Pre-parental	17	15	-0.643	0.005*
Parental	15	13	0.329	0.231

Correlations between Allelic Imbalance and Behavior

Brain Region	n	DF	R	p-value	Fisher's Z
AH	13	11	<0.001	0.999	0.183
IN	13	11	0.534	0.060	

Table S7. Allelic imbalance in the IN. The top part of this table shows the results of tests for allelic imbalance, or a ratio different from 1:1, in the expression of vasoactive intestinal peptide (*VIP*) alleles in the infundibular nucleus (IN). All tests were one-sample t-tests. The next two parts of the table shows the results of the correlations that were conducted on residual values calculated from the following statistical models: allelic imbalance & expression: sex + date + 1|year/qPCR run; allelic imbalance & behavior: sex + date + 1|year. See Figures 5, 10, S4, and S6 for corresponding plots of these data.

VIP Expression

Fixed Effect	n	DF	F-value	η^2	p-value
Morph	127	70	0.160	<0.01	0.690
Sex	127	70	3.811	0.05	0.055
Region	127	45	75.28	0.63	<0.001*
Morph:Sex	127	70	1.217	0.02	0.274
Morph:Region	127	45	12.17	0.21	0.001*
Region:Sex	127	45	11.54	0.20	0.001*
Morph:Region:Sex	127	45	1.840	0.04	0.182

Post-hoc tests for morph differences

Region	n	t-value	p-value
AH	59	-2.915	0.005
IN	68	2.145	0.037

Differences in Allelic Imbalance between Brain Regions

Fixed Effect	n	DF	F-value	p-value
Region	73	34	4.604	0.039
Sex	73	35	0.743	0.395
Region:Sex	73	34	0.849	0.363

Table S8. Interactions between morph, sex, and brain region in *VIP* expression. The results in this table are from MANOVA and *post-hoc* analyses that demonstrate the region-specific morph differences in vasoactive intestinal peptide (*VIP*) expression in the anterior hypothalamus (AH) and infundibular nucleus (IN), as well as the results of MANOVA tests for differences in allelic imbalance between the two brain regions. Overall expression data were $\log_2$ transformed and the allelic imbalance data were not transformed. The statistical model for the MANOVA analysis was as follows: Allelic imbalance ~ region + sex + 1|ID/Year. The statistical model for the ANOVAs was as follows: $\log_2$(VIP) ~ morph * region * sex + 1|ID/qPCR run. See Figure 6 for the plot corresponding with overall expression and Figure 8 for the plot corresponding with allelic imbalance.

Vasoactive Intestinal Peptide qPCR Assay

Gene	Primer Forward	Primer Reverse	Probe
VIP	AAGAAGCCAGGAAGAGCTAAAT	CTTTACCAGGTGTCCTTCAGAG	TTCTGTAGATGAGCTGCTGAGCCA
GAPDH	CATCACAGCCACACAGAAGA	CTCCAGTAGATGCTGGGATAATG	CTTCGGCATTGTGGAGGGTCTCAT
PPIA	GTGCCGAAGACAGCAGAAA	GCACATGAACCCAGGAATGA	TAGCCAAATCCCTTCTCACCAGTGC

Vasoactive Intestinal Peptide Allele-Specific qPCR Assay

Gene	Primer Forward	Primer Reverse	Probe
VIP^{2}	ATGTTGTGAAGTGAAAGTTGTG	GCTTTCAGTAGAGAATGCTAGA	TC+A+G+CTT+TTAT+T+A+CG
VIP^{2m}	ATGTTGTGAAGTGAAAGTTGTG	GCTTTCAGTAGAGAATGCTAGA	ATC+A+A+CT+TT+T+ATTA+C+GT

Table S9. Nucleotide sequences of primers and probes for RT-qPCR assays. The assays were designed and manufactured by IDT and/or IDT software. The vasoactive intestinal peptide (*VIP*) qPCR assay included two housekeeping genes, *GAPDH* and *PPIA*. The allele-specific qPCR assay was used to determine the degree of expression of the ZAL2^{m} allele of *VIP* (*VIP*^{2m}) relative to the ZAL2 allele of *VIP* (*VIP*^{2}). See Methods for more details.

Supplementary Figures

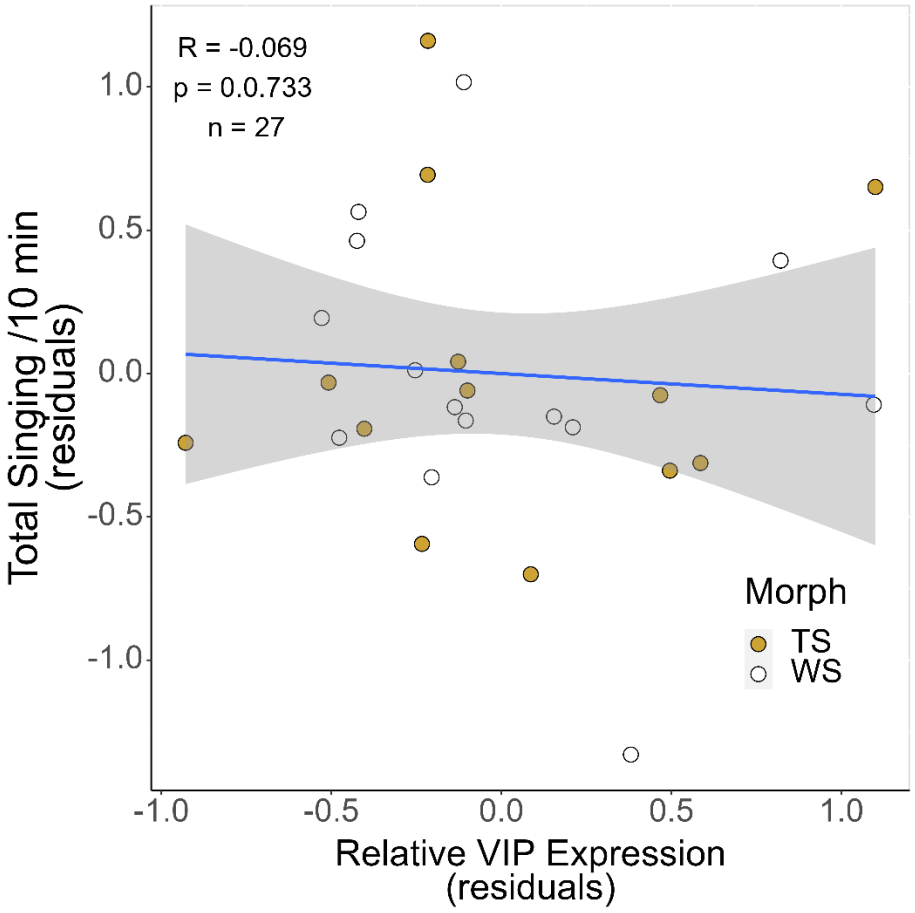

Figure S1. Correlation between *VIP* expression in the IN and territorial singing. In contrast with vasoactive intestinal peptide (*VIP*) expression in the anterior hypothalamus (Figure 2C), *VIP* expression in the infundibular nucleus (IN, x-axis) was not correlated with territorial singing (y-axis). See Table S3 for complete statistical results.

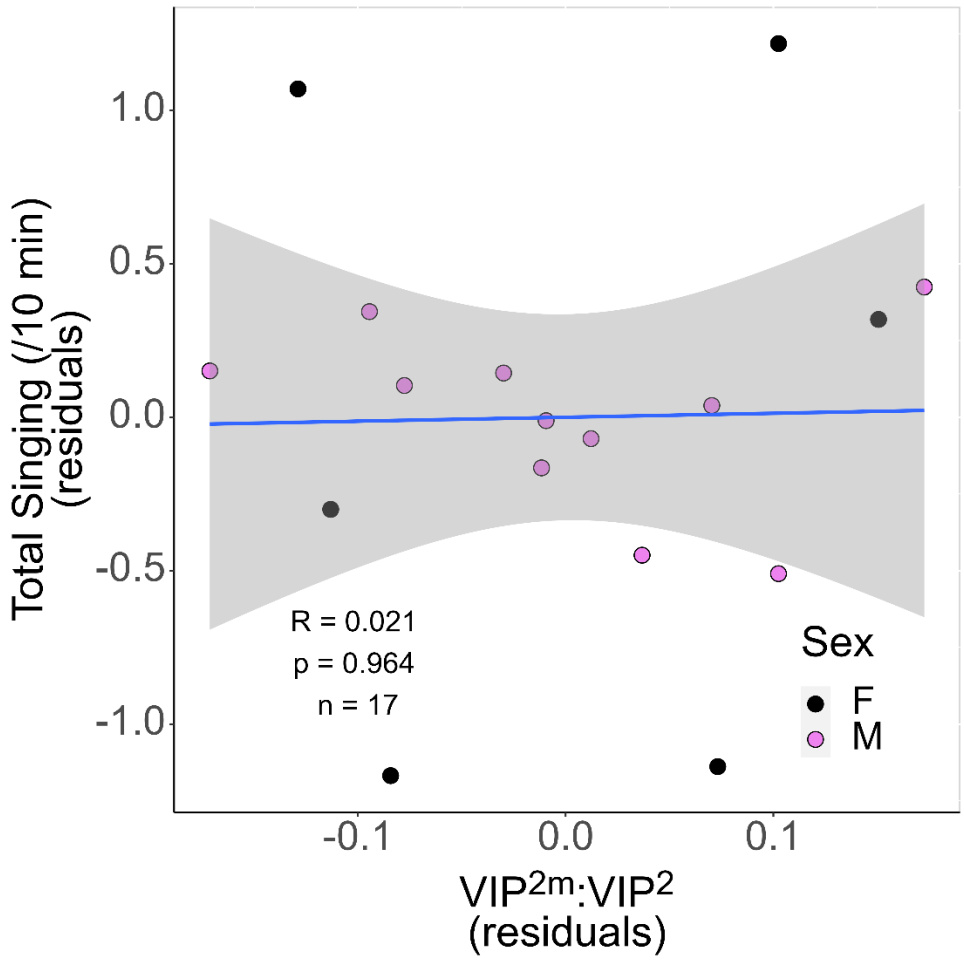

Figure S2. Correlation between allelic imbalance in the IN and territorial singing. In contrast with allelic imbalance in the anterior hypothalamus (Figure 3C), allelic imbalance in the infundibular nucleus (IN) was not correlated with singing rate. The color of each point corresponds with sex; violet is male (M) and black is female (F). All plotted values are residuals controlling for sex, date, and year. See Table S4 for complete statistical results.

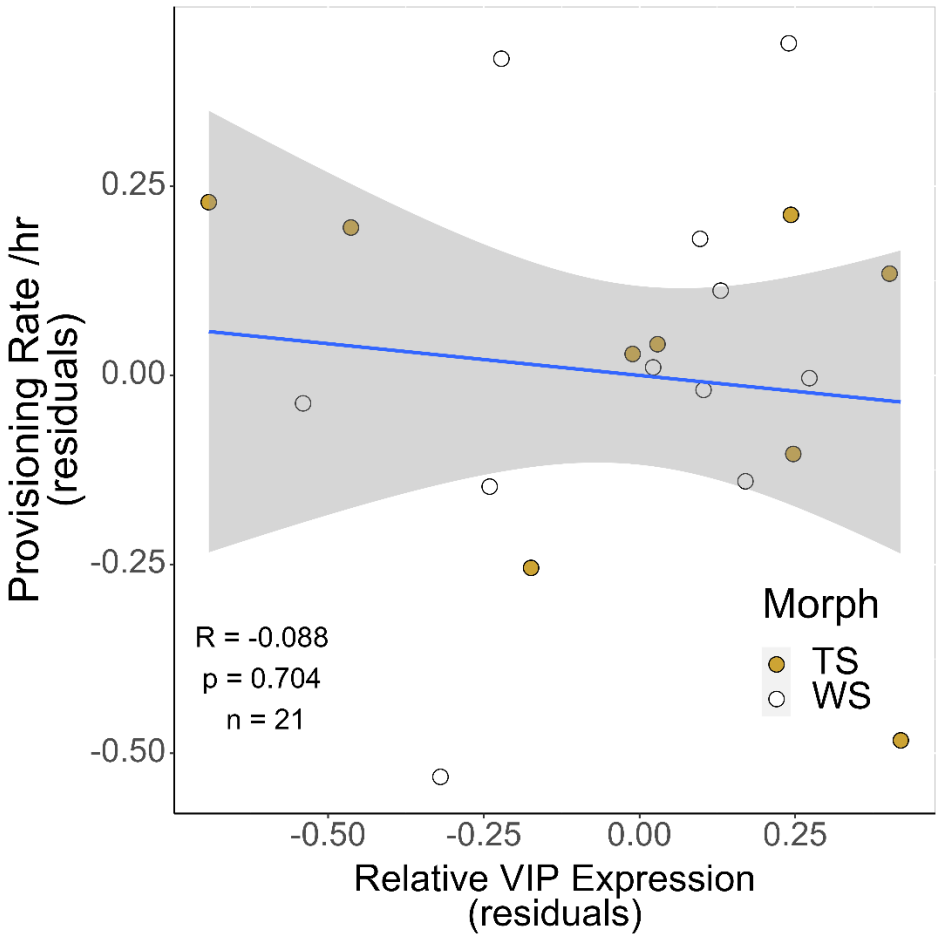

Figure S3. Correlation between *VIP* expression in the AH and nestling provisioning. In contrast with vasoactive intestinal peptide (*VIP*) expression in the infundibular nucleus (Figure 4C), *VIP* expression in the anterior hypothalamus (AH, x-axis) was not correlated with nestling provisioning (y-axis). See Table S5 for complete statistical results.

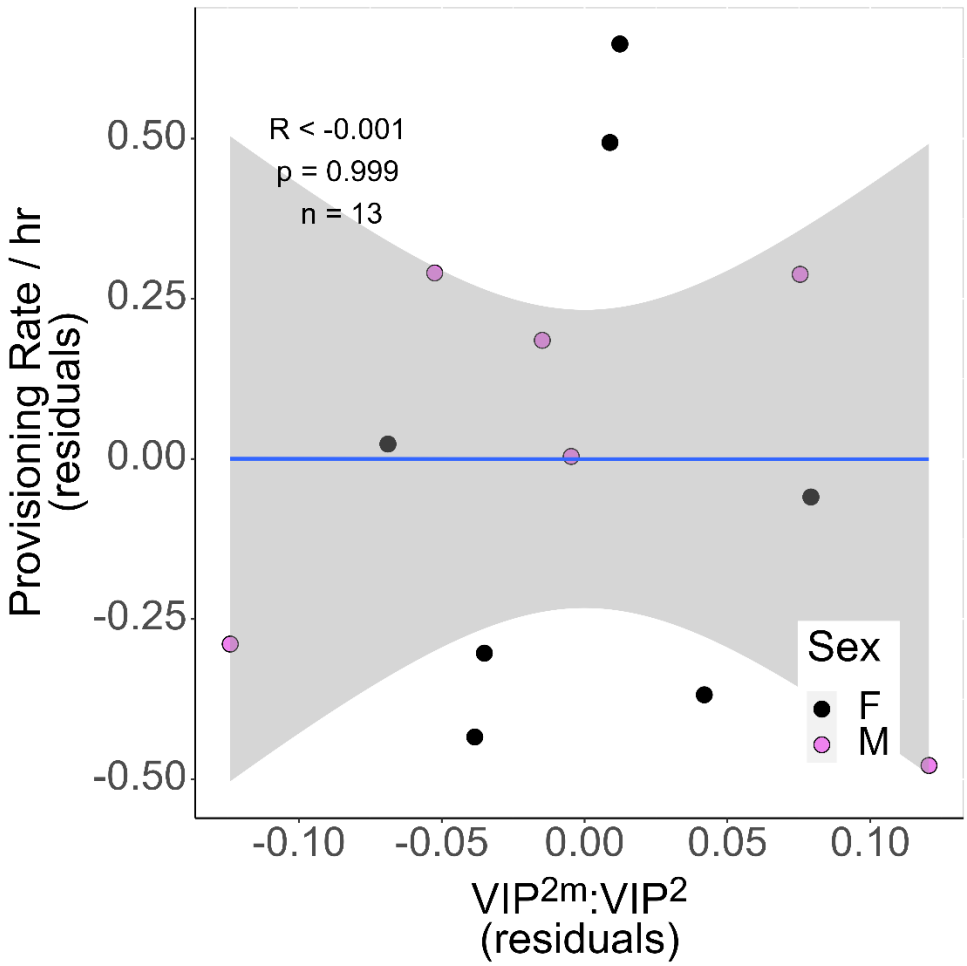

Figure S4. Correlation between allelic imbalance in the AH and nestling provisioning. In contrast with allelic imbalance in the infundibular nucleus (Figure 5C), allelic imbalance in the anterior hypothalamus (AH) was not correlated with provisioning rate. The color of each point corresponds with sex; violet is male (M) and black is female (F). All plotted values are residuals controlling for sex, date, and year. See Table S7 for complete statistical results.

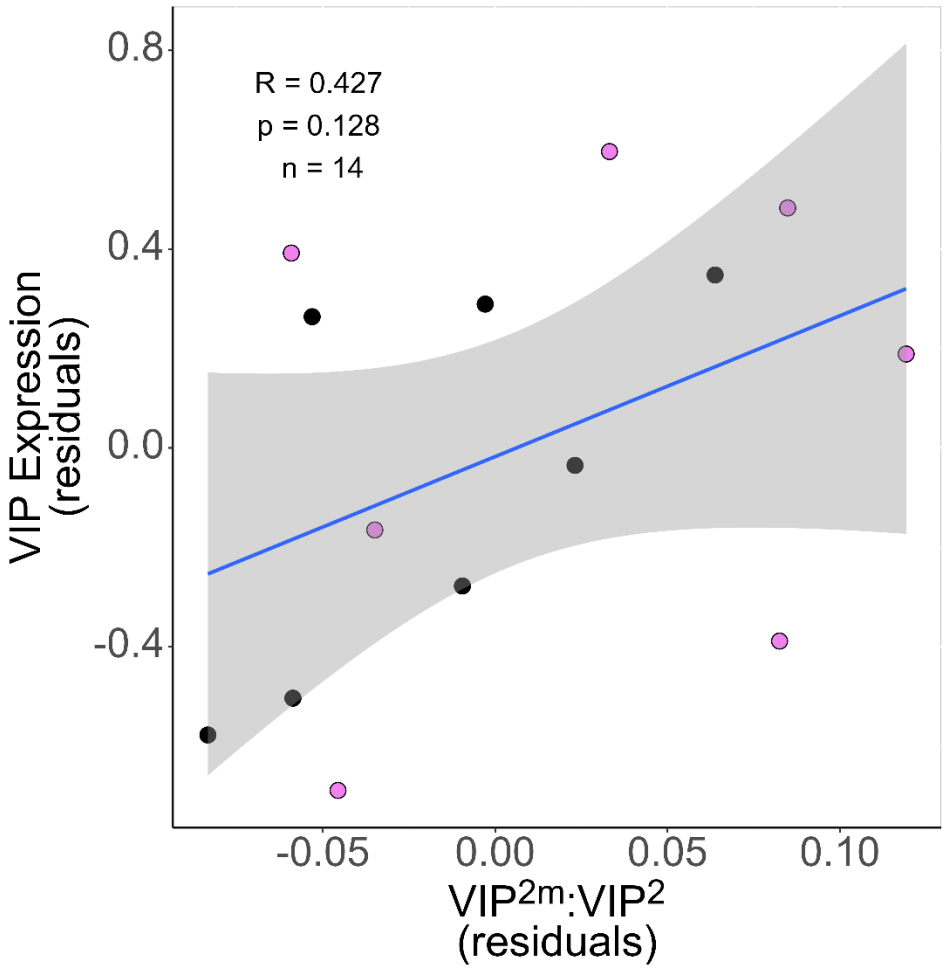

Figure S5. Correlation between allelic imbalance and overall *VIP* expression in the AH within the parental cohort. The correlation between the degree of allelic imbalance in the anterior hypothalamus (AH) and overall vasoactive intestinal peptide (*VIP*) expression in the AH was not significant within the parental cohort. The color of each point corresponds with sex; violet is male (M) and black is female (F). All plotted values are residuals controlling for sex, date, and year. See Table S4 for complete statistical results.

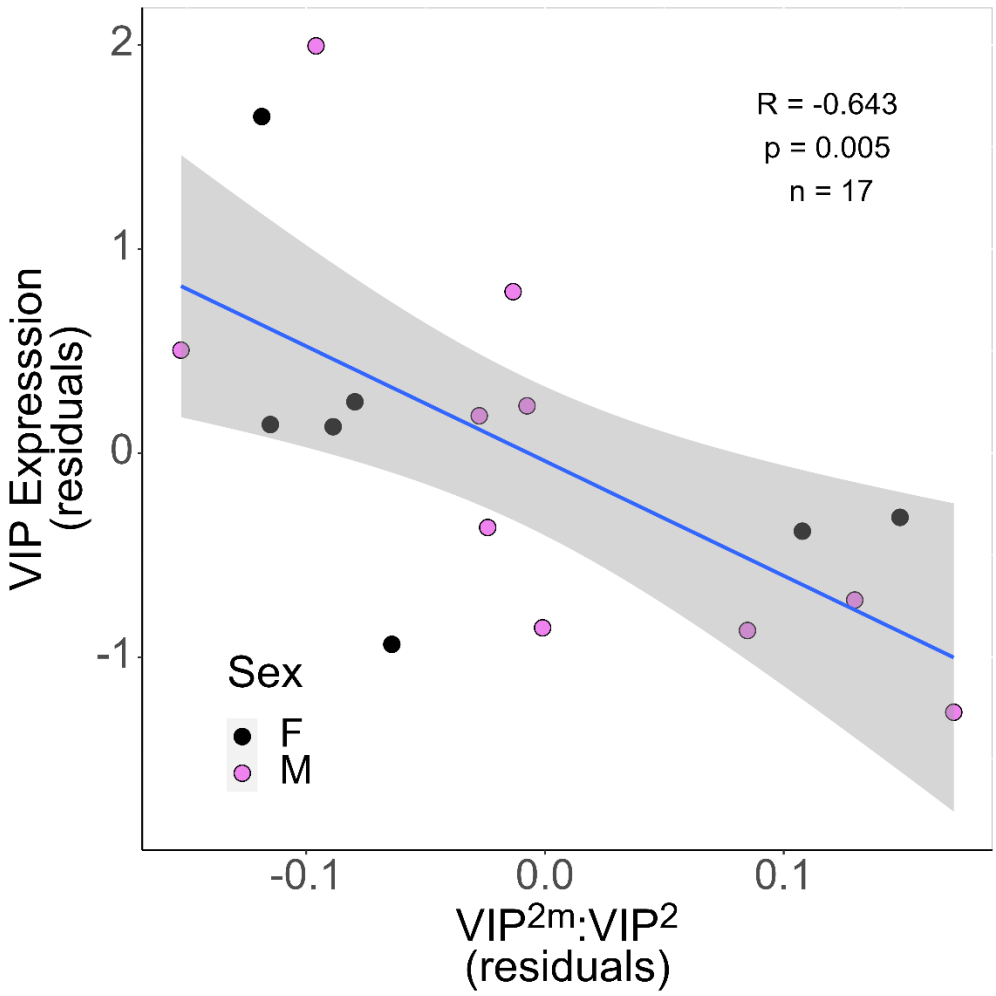

Figure S6. Correlation between allelic imbalance and overall *VIP* expression in the IN within the pre-parental cohort. The correlation between the degree of allelic imbalance in the infundibular nucleus (IN) and overall vasoactive intestinal peptide (*VIP*) expression in the IN within the pre-parental cohort was statistically significant. The color of each point corresponds with sex; violet is male (M), and black is female (F). All plotted values are residuals controlling for sex, date, and year. See Table S7 for complete statistical results.

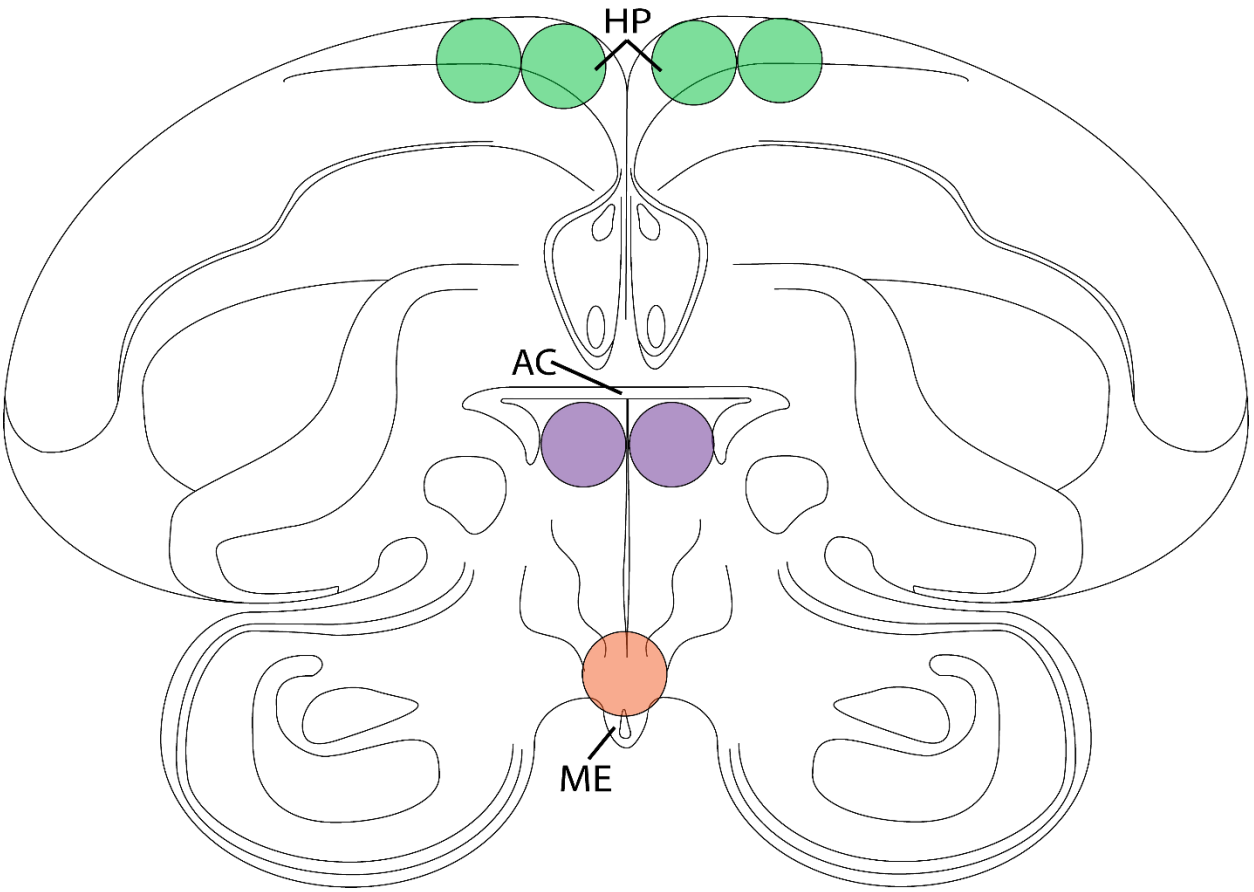

Figure S7. Anatomical locations of punches of the anterior hypothalamus and infundibular nucleus. Tissue samples containing vasoactive intestinal peptide (*VIP*)-expressing neurons were microdissected from brain tissue in order to extract RNA/DNA. The anterior hypothalamus (AH) was located using the anterior commissure (AC) as a landmark and bilateral punches 1mm in diameter (purple circles) were taken from two consecutive 200µm sections. The infundibular nucleus of the hypothalamus (IN) was located using the median eminence (ME) as a landmark. Punches 1mm in diameter, centered on the midline (orange circle), were taken from three consecutive 200µm sections. Punches of the hippocampus (HP) were also collected (1mm diameter, green circles) and used for inter-run calibration during qPCR. Illustration by M. R. Prichard.

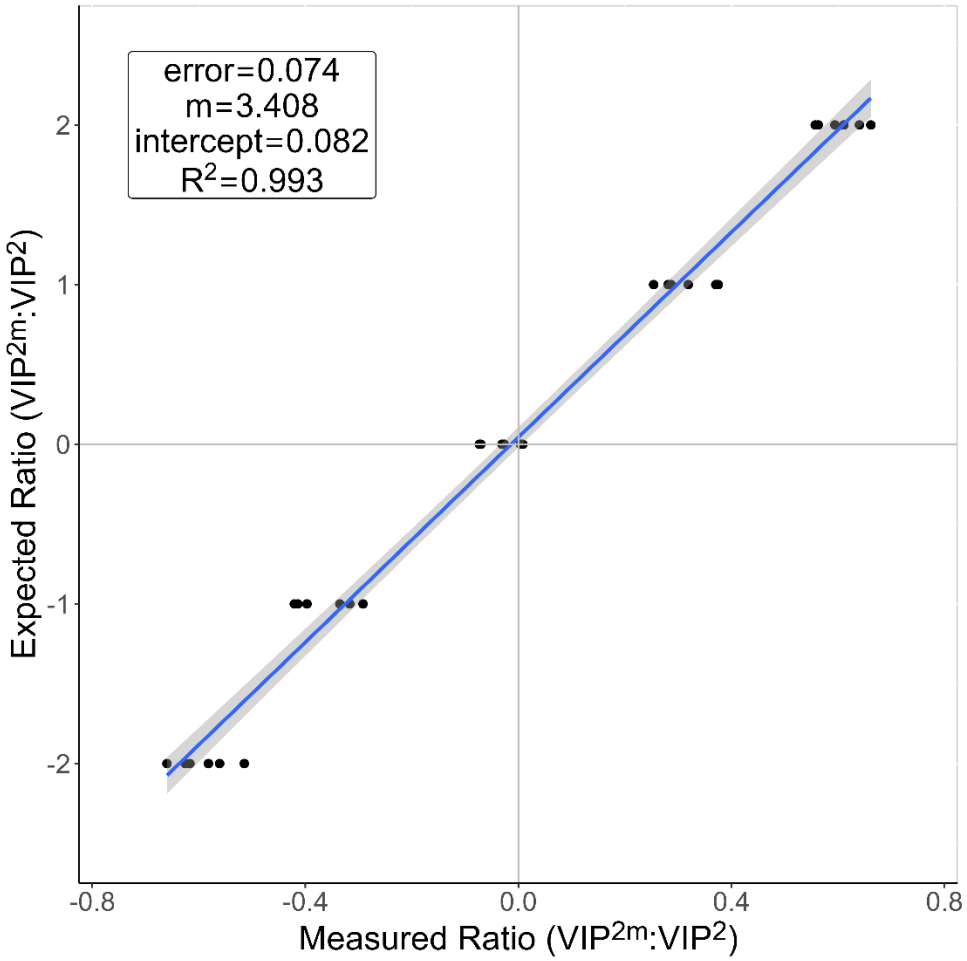

Figure S8. Standard curve used for the assay of allelic imbalance ($ZAL2^m$: ZAL2). The standard curve used for this assay was calculated from samples with known ratios of gDNA from ZAL2/ZAL2 and $ZAL2^m/ZAL2^m$ homozygotes, diluted in a linear fashion (1:8, 1:4, 1:2, 1:1, 2:1, 4:1, 8:1). Above, the x-axis indicates the ratios calculated from the samples in the standard curve and the y-axis indicates the expected ratio for each sample. The intercept and the R^2 suggest that the specificities of the two allele-specific probes were approximately equal across a range of allelic imbalance ratios. See Methods for more information.